Enhanced detection in hydroxylamine probe for the quantitative and qualitative analysis of S-acylated fatty acids on proteins

Final Degree Project

Biochemistry and Molecular Biology

Jahaciel Villaverde Nogues

Scientific director: Dra. Gemma Triola Guillem

Department of Chemical Biology (ChemBio)

Institut de Química Avançada de Catalunya (IQAC)

Academic tutor: Dr. Juan B. Fernández Larrea

Department of Biochemistry and Biotechnology

Universitat Rovira i Virgili

Universitat Rovira i Virgili

Tarragona, June 2025

Yo, Jahaciel Villaverde Nogues, con DNI 49317122Q, soy conocedor de la guía de prevención de plagio en la URV Prevención, detección y tratamiento del plagio en la docencia: guía para estudiantes (aprobada en julio de 2017) y afirmo que este TFG no constituye ninguna de las conductas consideradas como plagio para la URV.

Tarragona, 04 de junio de 2025

ACKNOWLEDGEMENTS

This work has been carried out in Chemical Biology department (ChemBio), at Institut de Química Avançada de Catalunya (IQAC), under the supervision of Dra. Gemma Triola Guillem and Dr Juan B. Fernández Larrea.

This thesis was financed by the project 2021SGR00504 (Chemical Biology of Lipids and Proteins) funded by AGAUR, Generalitat de Cataluña.

The author received a scholarship, JAE Intro ICU (JAEICU_24_01203) from CSIC.

I am thankful to Dr. Gemma Triola for encouraging me to pursue this line of research and for supporting me throughout the process, generously sharing her experience and knowledge. I am also deeply thankful to Alexandra, the PhD student who worked alongside me in the lab, guided me through every challenge, and taught me how to navigate the laboratory with confidence.

I would also like to express my gratitude to my parents and brother for their unconditional support through these years.

A special thanks also to my friends: Ariadna, Cinta, Lucia, Pau, Emma, and Ainhoa for these four unforgettable years, which I hope are only the beginning of many more to come.

Lastly, I want to thank Francesca, for her constant support, love and patients throughout this last's months. Her encouragement kept me going during the most challenging moments. Thank you for being my anchor: I'm incredibly lucky to have you by my side.

ABSTRACT

S-acylation is a reversible lipid modification that regulates protein localization, stability, and function, with key roles in signaling and disease. However, its study is limited by the low ionization efficiency of fatty acid hydroxamates (FAHs), released upon hydroxylamine cleavage. To improve detection sensitivity, FAHs were derivatized with pyridine-2-carbonyl chloride and 4,4-dimethoxypiperidine, enhancing their signal in HPLC-HRMS. This optimized method enabled robust quantitative and qualitative analysis of S-acylation, as demonstrated in the human Neuro-2a (N2a) cell line. This approach provides a powerful tool for investigating the heterogeneous S-acylome and its dysregulation in neurodegenerative diseases like neuronal ceroid lipofuscinosis (CLN1).

KEY WORDS

S-acylation, hydroxylamine, fatty acid hydroxamate, liquid chromatography, mass spectrometry, derivatization, ionization enhancement, lipidomics, Neuro-2a cells.

INDEX

FIGURE INDEX

ABBREVIATIONS

Table 1: Comprehensive List of Abbreviations Utilized Throughout the Text.

^{1}H NMR	Proton Nuclear Magnetic Resonance
^{13}C NMR	Carbon-13 Nuclear Magnetic Resonance
ABE	Acyl-Biotin Exchange
ACN	Acetonitrile
ANOVA	Analysis of Variance
APE	Acyl-PEG Exchange
CLN1	Ceroid Lipofuscinosis Neuronal 1
DCM	Dichloromethane
DMEM	Dulbecco's Modified Eagle Medium
DMSO	Dimethyl Sulfoxide
EtOAc	Ethyl Acetate
ESI	Electrospray Ionization
FA	Fatty Acid
FAH	Fatty Acid Hydroxamate
FBS	Fetal Bovine Serum
HPLC-HRMS	High Performance Liquid Chromatography – High Resolution Mass Spectrometry
IMS	Ion Mobility Spectrometry
LC	Liquid Chromatography
LOD	Limit of Detection
LOQ	Limit of Quantification
MeOH	Methanol
MS	Mass Spectrometry
Na_2SO_4	Sodium Sulfate
$NaHCO_3$	Sodium Bicarbonate
NH_2OH	Hydroxylamine
NIH	National Institutes of Health
NMR	Nuclear Magnetic Resonance
N2a	Neuro-2a (mouse neuroblastoma cell line)
nGF-SPE	Nanographite Fluoride Solid-Phase Extraction
PBS	Phosphate Buffered Saline
PEG	Polyethylene Glycol
PPAA	Propanephosphonic Acid Anhydride
PPT1	Palmitoyl-Protein Thioesterase 1
Q-TOF	Quadrupole Time-of-Flight
S/N	Signal-to-Noise Ratio
TEA	Triethylamine
TLC	Thin Layer Chromatography

1. INTRODUCTION

1.1 S-acylation

The S-acylation is the post-translational modification of a cysteine residue with a fatty acid (FA) via thioester bond. This lipid modification provides the proteins with hydrophobicity therefore drives their association with membranes or even specific membrane subdomains allowing these proteins to have a key role in the regulation of protein trafficking. It has also been described as essential for the modulation of multiple cellular processes, such as signal transduction and apoptosis. This modification is highly common and could potentially affect 10-20% of the whole human proteome, thus its importance is well established. As a result, changes in how S-acylation and deacylation work are being linked more and more to a variety of human health issues, including metabolic and inflammatory diseases, neurodegenerative conditions, and cancer (1).

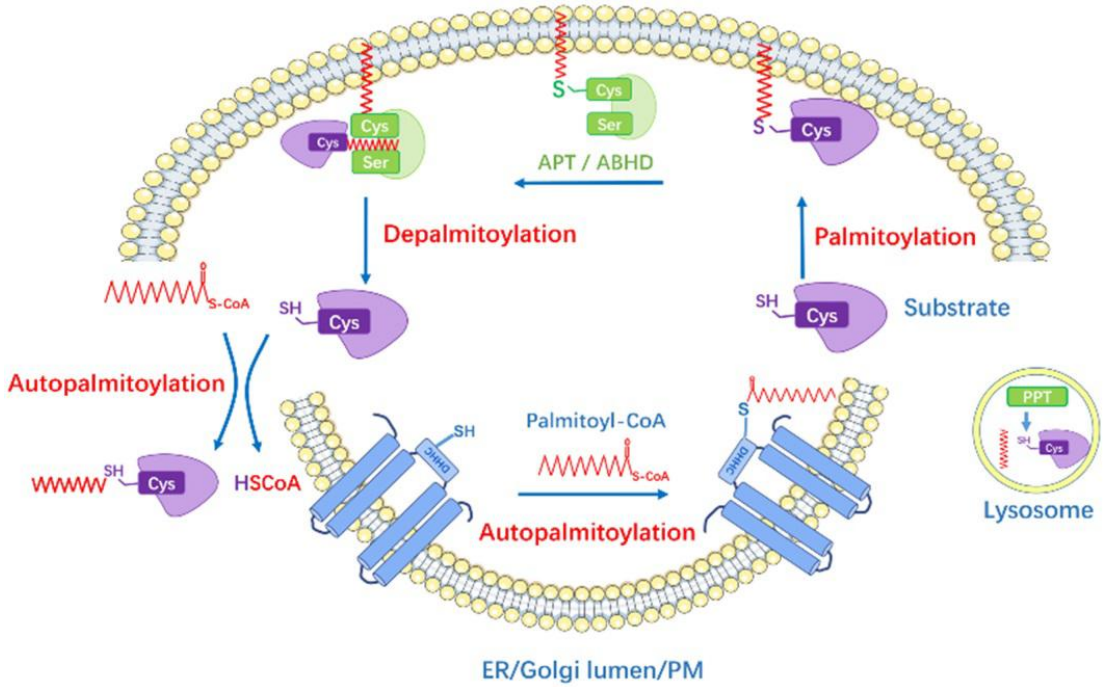

Figure 1: Scheme of the different S-acylation and deacylation pathways proteins can undergo (2).

Fatty acids can be attached to cytosolic cysteine residues within proteins by mediation of S-acyltransferases, mainly the transmembrane ZDHHC enzymes, named after the zinc finger containing Asp-His-His-Cys (DHHC) motif in their active site, which is essential for their catalytic function. The catalytic mechanism involves two steps: First, the DHHC enzyme's cysteine is auto-acylated via an acyl-CoA donor at the cytosolic CoA-binding site. Then, the acyl group is transferred to a cysteine on the substrate protein (1). In addition to this enzyme-mediated pathway, certain fatty acids can also spontaneously attach to cysteine residues through a non-enzymatic mechanism known as autoacylation. This involves reactive cysteine residues in the proteins which directly react with fatty acyl-CoA through thioester transfer reactions, highlighting that under specific conditions, S-acylation can proceed independently of ZDHHC enzymes (3).

This modification is reversible by deacylation, so it serves as a dynamic on/off switch, temporally controlling protein function. Deacylation enzymes are part of the serine hydrolase superfamily. These enzymes use a conserved serine to attack the thioester carbonyl in protein S-acylation, forming a transient ester intermediate that is then hydrolyzed to regenerate the active enzyme. Currently, there are few known deacylation enzymes which include acyl-protein thioesterase 1 (APT1) and APT2, palmitoyl protein thioesterase (PPT1) and some α\β-hydrolase containing-domain proteins (ABHD10, ABHD17). APT1 and APT2 are known cytosolic and Golgi-associated deacetylases, but the range of substrates in which they act is yet unclear. The ABHD17 family has emerged as an important group of deacetylases, particularly active at the plasma membrane. Selective inhibitors of ABHD17 confirm its role in regulating dynamic palmitoylation. Additionally, deacetylation activity has been detected within mitochondria, where APT1 is now recognized as functionally active, suggesting broader spatial regulation of this lipid modification (4)(5). Lastly, PPT1 is the only known deacylation enzyme which is involved on the lysosomal degradation of S-acylated proteins (1).

1.2 S-acylation functions

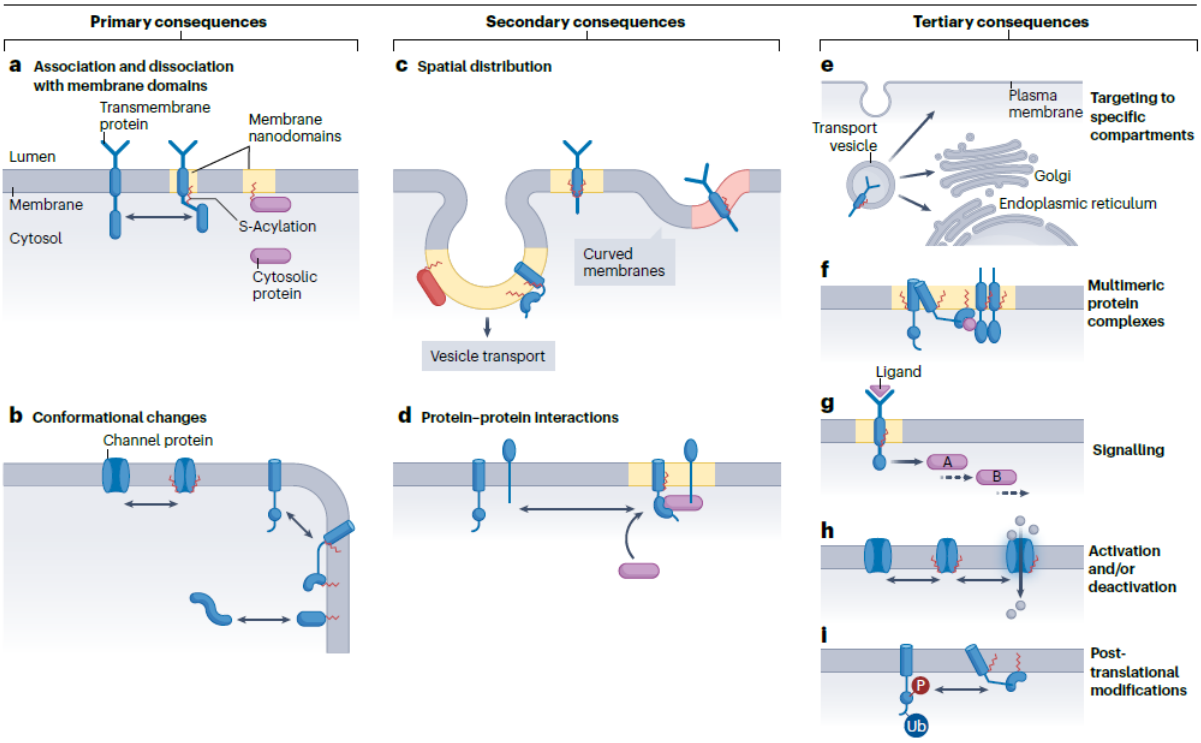

Figure 2: Scheme of the different functions S-acylation has on proteins and cell functioning (1).

One primary consequence of S-acylation is the promotion of protein association with specific membrane domains, particularly lipid nanodomains enriched in cholesterol and sphingolipids. Through this membrane anchoring, S-acylation not only facilitates the spatial targeting of soluble proteins but also modulates the partitioning of transmembrane proteins into distinct membrane subregions, which is essential for organizing membrane microenvironments critical for signal transduction and trafficking. One of the most well-studied examples of this is the GTPase Ras. Specific isoforms of Ras require palmitoylation for localization to the plasma membrane, where Ras becomes activated and signals to downstream effectors in the MAPK signaling pathway regulating cell growth and proliferation (6).

Additionally, S-acylation can induce conformational changes in proteins that influence their structural flexibility and activity. For example, S-acylation has been shown to regulate the gating kinetics of voltage-gated sodium channels, affecting their voltage sensitivity and inactivation properties, which in turn impact neuronal excitability and cardiac rhythm (7). Beyond direct structural modulation, S-acylation also influences the assembly of multiprotein complexes, acting as a molecular cue for the recruitment of signaling molecules to specific membrane interfaces. This property is critical in contexts such as the formation of

immunological synapses, neuronal synapses, and endoplasmic reticulum–plasma membrane contact sites, where the spatial and temporal coordination of signaling platforms depends on lipid modification of key scaffolding proteins (1).

Furthermore, S-acylation plays an integral role in regulating protein trafficking and subcellular localization. By promoting the incorporation of proteins into transport vesicles, S-acylation determines their directional movement through the endomembrane system, influencing their final destination at the plasma membrane, lysosomes, or other organelles. This mechanism is exemplified by the requirement of S-acylation for the export of certain receptors from the endoplasmic reticulum to the Golgi apparatus and subsequently to the cell surface. The reversible nature of this modification also allows proteins to undergo cycles of membrane association and dissociation, enabling fine-tuned regulation of their localization in response to cellular signals (8).

Another key functional outcome of S-acylation is its role in crosstalk with other post-translational modifications. By influencing or being influenced by phosphorylation, ubiquitylation, or S-nitrosylation, and other lipid modification such as myristoylation, S-acylation integrates into a complex network of modifications that collectively determine protein stability, activity, and interaction potential. This interplay contributes to cellular plasticity and adaptability under physiological and pathological conditions (9).

Taken together, the diverse functional outcomes imparted by S-acylation, ranging from membrane association and structural modulation to complex formation, trafficking, and modification cross-talk, highlight its central role as a versatile and dynamic regulator of protein function. Understanding these multifaceted effects is critical not only for elucidating basic cellular mechanisms but also for identifying potential therapeutic targets in diseases where dysregulated S-acylation contributes to pathogenesis.

1.3 S-acylation disorders and disease development

The dysregulation of the S-acylome in cellular context is critically important because dysregulated protein S-acylation has been implicated in the pathogenesis of a broad spectrum of human diseases across multiple systems (2).

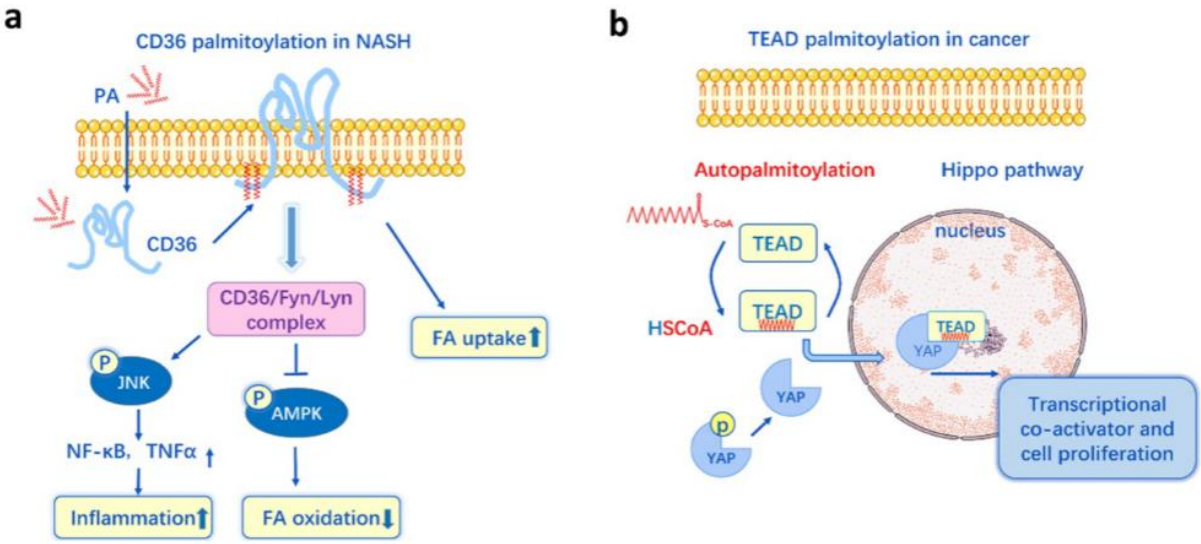

Figure 3: a: Increased palmitoylation of CD36 and its impact on NASH. **b:** TEAD autopalmitoylation enables YAP binding and Hippo transcriptional activity.

In metabolic disorders such as obesity, type 2 diabetes, and non-alcoholic steatohepatitis (NASH), aberrant acylation of key metabolic regulators like CD36, GLUT4, and eNOS disrupts fatty acid uptake, glucose metabolism, and endothelial function, contributing to insulin resistance, lipid accumulation, and vascular complications. In NASH, for example, increased palmitoylation of CD36 promotes CD36/Lyn/Fyn complex, impairing lipid uptake and inflammation, exacerbating liver fibrosis and steatosis (Figure 3a)(10). In diabetes, impaired acylation of GLUT4 affects glucose transporter trafficking, worsening hyperglycemia (11).

In cancer, dysregulated S-acylation plays a pivotal role in promoting tumor progression, metastasis, and resistance to therapy. Proteins such as epidermal growth factor receptor (EGFR), programmed death-ligand 1 (PD-L1), and TEAD transcription factors undergo acylation that enhances their stability, activation, and oncogenic signaling. For instance, increased acylation of EGFR supports dimerization and kinase activation, driving proliferation in non-small cell lung cancer, while acylation of PD-L1 stabilizes its expression, enabling immune evasion by tumor cells in breast and bladder cancers (12)(13). Furthermore, acylation of TEAD is required for its interaction with YAP/TAZ, key effectors of the Hippo pathway involved in cell growth and survival; hyper acylation of TEAD has been linked to enhanced oncogenic signaling in prostate and liver cancers(Figure 3b)(14).

In neurodegenerative diseases such as Alzheimer's, Parkinson's, and Huntington's disease, abnormal S-acylation alters the function and localization of critical neuronal proteins, leading to synaptic dysfunction and neurodegeneration. In Alzheimer's disease, hyper acylation of amyloid precursor protein (APP) and β-secretase (BACE1) enhances amyloidogenic

processing, increasing toxic β-amyloid accumulation (15). In Parkinson's disease, acylation defects in α-synuclein and MAP6 proteins have been linked to protein aggregation and neuronal toxicity, and an upregulation of their S-palmitoylation has been describe as a possible therapeutic strategy (16). Similarly, in Huntington's disease, the inhibition of APT1 enhanced S-acylation, and increased the vesicular transport of BDNF reversing neuropathology, locomotor deficits, and anxio-depressive behaviors (17).

In the immune system, abnormal acylation influences inflammatory and autoimmune responses. Acylation of MYD88, a critical adaptor in Toll-like receptor (TLR) signaling, enhances downstream activation of NF-κB and MAPK pathways, increasing cytokine production and contributing to chronic inflammation. In models of sepsis, hyper acylation of MYD88 worsens inflammatory injury, while inhibition of its acylation improves neutrophil function and survival. Acylation also modulates innate immune sensors like STING and TLR2, where dysregulated acylation affects antiviral responses and susceptibility to infection. In viral infections, such as hepatitis C virus, chikungunya virus, and HIV, viral replication depends on host protein acylation machinery, with viral proteins requiring acylation for membrane targeting and assembly. Interestingly, inhibitors targeting these pathways can reduce viral replication and pathogenicity (2).

In the nervous system, acylation of synaptic proteins plays a fundamental role in neuronal communication and plasticity. Excessive acylation of AMPA receptor subunit GluA1 following a high-fat diet impairs its phosphorylation and trafficking, leading to cognitive deficits and hippocampal dysfunction. Palmitate-induced acylation also increases the activity of the acyl transferase ZDHHC3, which further alters synaptic protein regulation in diet-induced cognitive decline (18). Proteins such as PSD-95, NR2A, NR2B, and GABA_A receptor subunits rely on balanced acylation for proper synaptic localization and receptor clustering; dysregulation of their acylation has been associated with schizophrenia, depression, and anxiety disorders (18)(19). In depression, reduced acylation of serotonin 1A receptor (5-HT1AR) correlates with altered receptor signaling and has been observed in individuals with major depressive disorder and suicide victims (20).

Altogether, the study of the cellular S-acylome is vital because it provides insight into how aberrant acylation of diverse proteins contributes to the molecular pathology of metabolic, neurodegenerative, inflammatory, infectious, autoimmune, and neoplastic diseases. Mapping the S-acylome not only enhances our understanding of disease mechanisms but also identifies

novel biomarkers and therapeutic targets for pharmacological intervention aimed at restoring normal protein acylation and cellular homeostasis across a wide range of human disorders.

1.4 The heterogeneous S-acylome

Palmitic acid is the most common fatty acid bound to cysteine residues. In consequence, S-acylation is also referred as S-palmitoylation or palmitoylation, even when the specific lipid attached is not palmitic acid (C16:0). It has been proven but that S-acylation include a vast range of FA which can be covalent bonded by thioester bond such as myristic acid (C14:0), palmitate (16:0), palmitoleate (16:1), stearate (18:0), oleate (18:1), and arachidonate (20:4) (21)(22). Furthermore, an increasing amount of evidence indicates a link between heterogeneous acylation and various functional outcomes. In fact, studies have shown that proteins modified with unsaturated fatty acids exhibit higher insertion rates into membranes and a greater tendency to cluster (23).

The vast majority of these past mentioned studies only focus on the S-acylation with palmitic acid (C16:0), it's binding sites on the protein or in the behavior of the mechanisms of palmitoylation including the enzymes that acylate and deacylate the substrate proteins. However, it has been proven that S-acylation is a heterogeneous modification that includes a significant variety of FA, from short chains to long chains, saturated or unsaturated. How the involvement of these different modifications results in different functional outputs is just starting to be explored (24).

Initial studies have demonstrated that the incorporation of unsaturated fatty acids into proteins significantly modifies their biophysical behavior within cellular membranes. Specifically, these modifications have been associated with a higher rate of membrane insertion compared to their saturated counterparts, as well as an increased propensity to form microdomains or clusters. This suggests that the degree of unsaturation in lipid modifications plays a critical role in determining the spatial organization and functional dynamics of membrane-associated proteins (23).

Moreover, modifications of signaling proteins with unsaturated or polyunsaturated fatty acids have been shown to significantly impact their membrane localization and downstream signaling capacity. For instance, when the Src-family kinase Fyn is modified with unsaturated or polyunsaturated fatty acids, its association with lipid rafts is diminished, leading to a reduction in T-cell signal transduction (25). More recent findings have revealed that both

palmitate and oleate can coexist on a single residue of the GNAI protein. This heterogeneous fatty acid composition carries important functional implications: specifically, only oleoylation effectively disrupts epidermal growth factor receptor (EGFR) signaling by displacing GNAI from detergent-resistant membrane fractions (26).

1.5 S-acylation study methods

Many previous findings on the field of S-acylated proteins have relied on metabolic labeling strategies using radioactive or azide/alkyne-tagged fatty acids. One of the first techniques to study S-acylation was the use of radioactive [^{3}H]-palmitate, which can be incorporated into cells proteins by lipid metabolic labeling (LML), followed by quantification by autoradiography. From this point, several probes were developed, including those with varying chain lengths, levels of unsaturation or isotopes [^{3}H] [^{14}C] [^{125}I]. This kind of probes but, has a wide range of limitations that significantly limits the current use of this technique, such as the requirement of long exposure times (days to weeks), the weakness of the signals, the hazard of the reagents employed, and the difficulty to apply this approach to the study of the proteome (27)(28).

Another typical approach for the study of S-acylation is the use of click chemistry strategies after metabolic labeling with azide/alkyne-tagged fatty acids. Thus, the modified lipids are taken up by cells and incorporated into proteins, which can then be tagged with biotin or fluorescent markers for detection via gel electrophoresis, Western blotting, fluorescence microscopy, or enriched to be identified by mass spectrometry (MS)-based proteomics (29).

Alkyne-based probes like 17-ODYA and 15-HDYA are commonly used due to lower background and better labeling efficiency compared to azide-based ones. This technique enables large-scale identification of S-acylated proteins and the study of lipid turnover, enzyme activity, and lipid selectivity (30).

However, although tagged fatty acids are more sensitive than radiolabeled probes and easier to handle, there are several drawbacks associated to both of these techniques. As an example, it cannot be used to identify the exact site or type of lipid modification, because these probes can be metabolized to longer or unsaturated fatty acids (31) and it can be also incorporated into proteins by other means such as O-acylation or N-myristoylation (32). Besides, the exogenous addition of non-natural fatty acids may influence the intracellular lipid levels in the sample. Moreover, the natural lipids found in the cells compete with these modified lipids for the

modifications of proteins and this might lead to poor labeling of proteins with a rapid turnover compared to those with a more stable palmitoylation state or in cell lines with a high lipogenic activity (*de novo* fat synthesis) (31). Finally, it fails to identify S-acylation with different FA than those exogenously added.

In addition to metabolic labeling, Acyl-biotin exchange (ABE) is one of the most widely used methods for enriching and identifying S-acylated proteins and peptides. It operates through a three-step chemical protocol: first, free thiols in the sample are blocked using reagents such as N-ethylmaleimide (NEM); second, hydroxylamine is applied to selectively cleave thioester bonds, thereby exposing new thiols; and third, these newly revealed thiols are labeled with thiol-reactive biotin compounds. This labeling enables the isolation of S-acylated proteins using streptavidin-based enrichment, after which they can be analyzed by techniques such as Western blotting or mass spectrometry (33).

Several variants of ABE have been developed to improve its performance. For example, Acyl-RAC replaces biotin tagging with thiol-reactive resins, simplifying the protocol and reducing costs (34). Another variant, APE, uses PEG molecules to label the cleaved thiols, introducing a measurable mass shift that allows the relative quantification of S-acylation via gel electrophoresis or Western blot. These adaptations have made ABE a valuable tool in both targeted and proteome-scale studies (35).

However, the method has notable limitations. One major issue is the non-specificity of hydroxylamine for just thioesters bonds with fatty acids. As a result, proteins modified through other thioester linkages may be mistakenly identified as S-acylated, leading to false positives. This contributes to high background signals, which can mask the detection of low-abundance proteins. Incomplete blocking of free thiols in the initial step further exacerbates background noise. Additionally, the protocol involves multiple precipitation and wash steps that can result in sample loss and extended processing times (36).

Despite all these techniques that have been developed over the decades, as we mentioned, they have diverse disadvantages that could still be addressed. With exception of few cases, most of the techniques are protein-centered and as a result, they lose information about the lipid moiety attached to the S-acylation site due to the hydroxylamine treatment or by the exogenous addition of lipid probes. As a result, methods allowing direct analysis of the fatty acids linked to proteins under endogenous conditions would be preferred (21).

Recent studies have introduced new methods aimed at characterizing the attached fatty acids. One approach, using nanographite fluoride solid-phase extraction (nGF-SPE), enabled the identification of intact S-acylated peptides with diverse lipid moieties, including myristate, palmitoleate, and octanoate, indicating the complexity in lipid composition of modified proteins (37). Another study optimized sample handling to prevent thioester cleavage, allowing the detection of S-acetylation, a novel cysteine modification linked to acetyl-CoA, with potential roles in metabolism and tissue-specific regulation (38).

Despite these advances, technical challenges remain. Neutral hydroxylamine can cleave thioester bonds while preserving fatty acid identity by converting them to fatty acid hydroxamates (FAH), but efforts to characterize these products have faced limitations. Early attempts using gas chromatography-mass spectrometry (GC-MS) suffered from low sensitivity(39). Alternative strategies, such as hydrogenation with platinum oxide to form ethyl esters, can cleave thioesters but also risk altering the structure of unsaturated fatty acids, thereby complicating analysis. These challenges underscore the need for more refined techniques to accurately map the full spectrum of lipid modifications in S-acylation without compromising molecular integrity (40).

1.6 Group findings (Hydroxylamine probe)

It is at this point, that our group reported, a Liquid Chromatography (LC)-MS method for the identification of S-linked fatty acids based on the capability of NH2OH to selectively cleave thioester bonds and generate the corresponding fatty acid hydroxamates (FAH) that could later be analyzed through LC-MS. However, the initial method relied on a hydroxylamine fluorescent derivative, and it required large amounts of this challenging synthetic compound. All this difficulted its wide application and further optimization (23).

Figure 4: General protocol for the qualitative and quantitative analysis of S-acylated proteins in cell lysates.

Later on, a much easier and general protocol was developed based on the hydroxylamine (NH_2OH) (Figure 4). Briefly, the sample from *in vitro* or *in vivo* origin, is lysed and its proteome is precipitated using an organic solvent mixture together with a centrifugation step, this is followed by the reaction with NH_2OH to release the corresponding S-linked fatty acids as fatty acid hydroxamates (FAH) that are now extracted with a water-methanol-chloroform mixture. Finally, the organic phase containing the FAHs is evaporated to dryness, diluted in MeOH and injected into the LC-HRMS instrument for its analysis, where we can distinguish all FAH by its mass and its relative quantification. Further on, to make this method not only semiquantitative but totally quantitative, a C19:0 FAH is added before the lipid extraction in a known concentration, as this FA is not found naturally in living organisms and so does not interfere with the analysis of the S-acylome (21).

This new developed technique provides a straightforward method for the quantitative and qualitative analysis of the heterogeneous pool of FA attached to proteins via S-acylation. Moreover, the fact that this molecule is cheap and commercially available facilitated its implementation for the wide screening of different cells and tissues. In addition, this method could also be used for the analysis of heterogeneous S-acylation of specific proteins and not only the tissue pool if this is coupled with immunoprecipitation and posterior cleavage with NH_2OH. However, even with all the advances and benefits this method provides, methods to improve the mass-based detection of the resulting FAH would be desirable to enhance the sensitivity of the method and its applications.

1.7 Mass spectrometry low ionization

Mass spectrometry (MS) is a key analytical technique widely used in fields such as proteomics, lipidomics, and metabolomics (41). The choice of ionization method depends on the sample and analytical goals, with techniques generally classified as hard (high energy, causing fragmentation) or soft (low energy, preserving molecular integrity). Electrospray ionization (ESI), commonly coupled with liquid chromatography (LC), is the most widely used soft ionization method in chemical and biochemical analyses. It involves generating multicharged droplets, evaporating the solvent, and releasing ions into the gas phase through Coulombic repulsion (Rayleigh limit), followed by separation by mass-to-charge ratio in the mass analyzer (42)(43).

Fatty acid hydroxamates (FAH) can be detected in both positive and negative ionization modes (44). However, they are low-polar compounds, with reduced ionization properties.

Furthermore, their known chelating ability, which is sometimes extremely useful, for example for the extraction of iron (III) from aqueous samples or their poor solubility in organic solvents can also hamper their appropriate detection by mass spectrometry (45).

Compounds that exhibit a low ionization efficiency in solution are not desirable for ESI-MS techniques since their detection and quantification will be more complex and not completely accurate. In these cases, introducing a step of chemical derivatization of the analyte is a widely employed technique to enhance their ionization, thereby facilitating their detection via mass spectrometry and the sensitivity and accuracy of the method (46). This process involves transforming the original molecule by adding or changing a functional group with the final goal of enhancing its properties such as volatility, stability or ionization efficiency.

When choosing a good derivatization reaction or reagent, several important characteristics must be considered to ensure the analytical process is effective and reliable. The reagent should introduce or enhance a functional group that enables detection. For precolumn derivatization, the reaction must be quantitative or nearly so, free of by-products, and must not negatively impact chromatographic separation. Moreover, the derivative should be stable, and if the reagent or its by-products interfere with detection, there must be a simple means to remove them. Reagents should ideally react specifically and selectively with the functional group of interest and operate under mild, controllable conditions. (46).

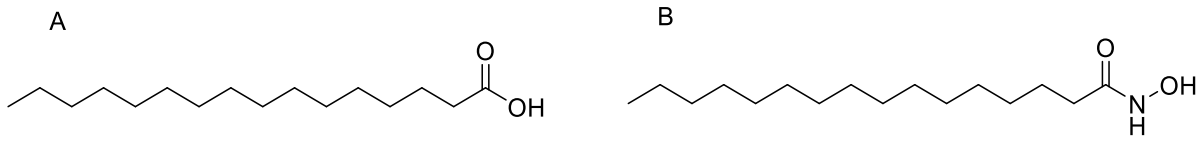

Figure 5: A: Fatty acid (Carboxylic acid). **B:** Fatty acid hydroxamate (Hydroxamic acid).

Fatty acid hydroxamates are structural analogues of fatty acids in which the terminal carboxylic acid group is replaced by a hydroxamic acid functional group (Figure 5). However, examples of methods to enhance the mass spectrometric detection of hydroxamic acid are currently lacking. Therefore, the initial aim of this work was to explore methods to enhance the mass-based detection of FAH with the ultimate goal of facilitating the study of S-acylated proteins. This goal involves identifying well-characterized derivatization reactions involving hydroxamic acids that proceed under mild conditions, offer high yields, and produce stable products suitable for analytical application.

One of these well described reactions is the acylation of hydroxamic acids with acyl chloride to form O-acylhydroxamates (47). The high yield of this reaction, the low formation of side products, and most importantly, the capability to add different functional groups in the acyl reagent that enhance the mass-detection of the hydroxamates suggest that this reaction could be employed as an optimal derivatization strategy to improve the analysis of FAH.

The subsequent phase involves identifying a structure that, when covalently attached to the hydroxamate, enhances its detection sensitivity in mass spectrometry. This enhancement is primarily achieved through the incorporation of molecular structures that are either pre-charged or readily ionizable under electrospray ionization (ESI) conditions. In positive ionization mode, commonly employed ionization-enhancing functionalities include tertiary amines, quaternary ammonium groups, and pyridinium rings (48).

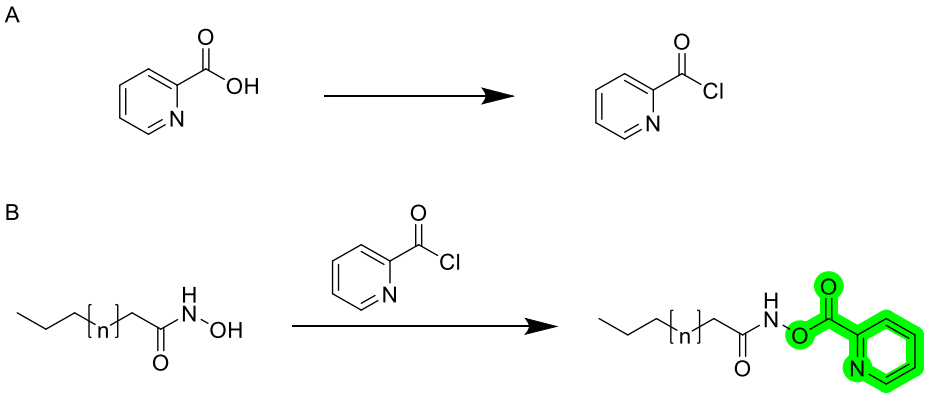

Figure 6: A: Pyridine-2-carbonyl chloride from 2-picolinic acid. **B:** Derivatization strategy via acylation of FAH.

Among these, the pyridyl group present in 2-picolylamine has demonstrated exceptional performance. Specifically, its use in the derivatization of carboxylic acids and dafachronic acid resulted in a reported 9 to 158 fold increase in detection sensitivity(49). 2-picolylamine features an aromatic pyridine ring bearing a tertiary amine, the primary functional molecular structure responsible for enhancement due to its favorable ionization properties (48).

Given that the primary objective is to preserve the ionization-enhancing structural motif, we have selected pyridine-2-carbonyl chloride (Figure 6A) as the derivatizing agent. This compound retains the key pyridyl structure responsible for improved ionization, while replacing the primary amine with an acyl chloride group, which is more suitable for acylation of hydroxamic acids (Figure 6B). Pyridine-2-carbonyl chloride is commercially available and

can also be readily synthesized from 2-picolinic acid through standard laboratory procedures (Figure 6A).

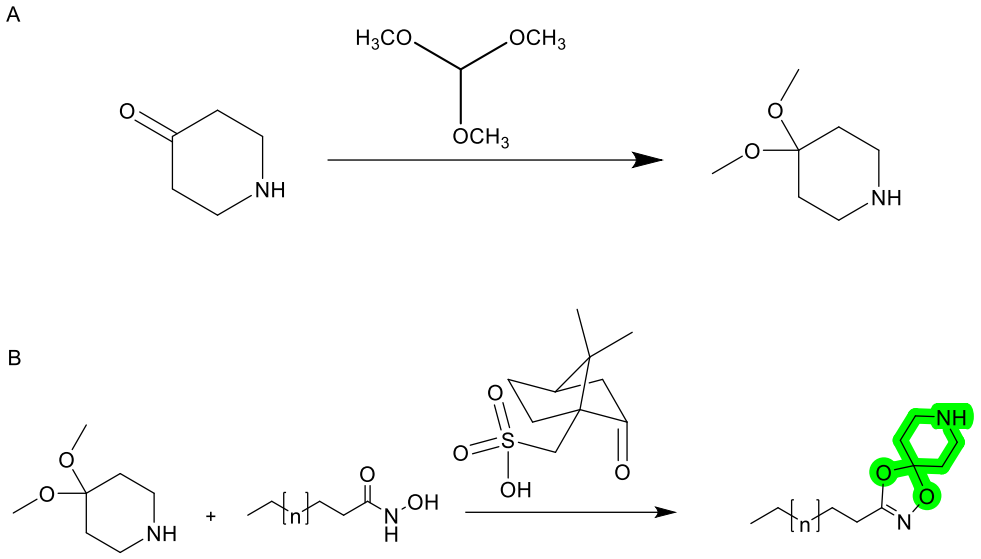

Figure 7: Simplified reaction steps. **A:** Formation of the ketal group as part of the synthesis of the enhanced mass-detection molecular structure. **B:** Transketalization reaction proposed for the derivatization of FAH.

Another reaction investigated in this study was the formation of 5,5-dimethyl-1,4,2-dioxazoles through the transketalization of 2,2-diethoxypropane with a hydroxamic acid, which has been previously employed as a protecting group for hydroxamic acids (50). Transketalization is typically carried out under mild conditions, proceeding as a one-step reaction overnight, making it well-suited for derivatization purposes (Figure 7B).

By modifying the substituents of the ketal moiety, it is possible to introduce a molecular structure that enhances mass spectrometric detection. In this case, 4,4-dimethoxypiperidine was incorporated, a cyclic hexane derivative bearing a secondary amine. The use of secondary amines as derivatization reagents in LC-MS significantly enhances analyte detectability, with reported sensitivity improvements ranging from 50 to 1500-fold. This enhancement is primarily due to increased ionization efficiency and improved chromatographic behavior(51). This product is derived from 4-piperidone through a well-established reaction that proceeds under mild conditions, typically completed overnight (Figure 7A) (52).

However, this latter option was quickly discarded due to the low reaction yield (11%) and the formation of numerous undesired byproducts, which were characterized via mass spectroscopy (Annex 1) and had been previously reported in the literature. (53).

1.8 Study and hypothesis

In this study, we evaluated the effectiveness of pyridine-2-carbonyl chloride and 4,4-dimethoxypiperidine as derivatization reagents for fatty acid hydroxamates (FAHs) to improve their detection sensitivity in high-performance liquid chromatography coupled with high-resolution mass spectrometry (HPLC-HRMS). Maintaining the quantification characteristic of the previous studies. Enhancing the sensitivity and accuracy of this analytical probe holds significant potential for advancing the comprehensive investigation of the S-acylome, particularly in the context of diseases associated with dysregulated S-acylation.

For this purpose, we synthetized the final derivatization products and compared their signal in the LC-MS, but we also tested its effectiveness in the characterization of the S-acylome in N2a cells.

As at this moment in this research group we are studying the neuronal ceroid lipofuscinoses (NCLs) which are a group of rare, fatal, genetically inherited lysosomal disorders that primarily affect the nervous system, leading to progressive deterioration in vision, movement, and cognitive abilities. There is currently no cure, and affected children die prematurely. There are 14 known types of NCLs, classified by the gene mutation and age onset (CLN1 to CLN14), with CLN1 and CLN3 mutations being the most common 1 (54).

CLN1 is associated with a deficiency in the enzyme palmitoyl-protein thioesterase 1 (PPT1), which is crucial for the lysosomal degradation of S-acylated proteins. PPT1 impairment results in abnormal storage of proteins and lipids in neurons, causing the symptoms of CLN1 disease to develop (55).

N2a cells have been widely used in neurodegenerative research due to their neuronal origin and capacity to differentiate. Their use in modeling various neurodegenerative diseases, including lysosomal storage disorders and protein misfolding conditions, makes them a valuable tool for studying CLN1/PPT1. Their established role in neurodegeneration research supports their application in exploring disease mechanisms and potential therapies (56).

2. OBJECTIVES

In this work, we want to explore different derivatization strategies for fatty acid hydroxamates (FAH) to enhance its detection sensitivity in HPLC-HRMS. Focusing on its application to the study of the S-acylation PTM and proving its effectiveness with the characterization of the S-acylome of N_2a cells for the study of neurodegenerative diseases regulated by S-acylation.

Therefore, in this work:

- Synthetize, analyze and validate the derivatized products from fatty acid hydroxamates (FAH) with pyridine-2-carbonyl chloride and 4,4-dimethoxypiperidine.

- Test the properties of the derivatized product with the best derivatization agent as suitable for the quantitative and qualitative analysis of FAH.

- Assess and optimize the improvement of the probe with the derivatization step on N2a cell line to characterize its S-acylome.

3. MATERIALS AND METHODS

Chemicals

Fatty acids C8:0 (Caprylic acid), C14:0 (Myristic acid), C16:0 (Palmitic acid), C16:1 (Palmitoleic acid), C19:0 (Nonadecanoic acid), C22:1 (Erucic acid)(All fatty acids from TCI), 4-piperidone hydrate hydrochloride (TCI), p-toluenesulfonic acid monohydrate (Sigma-Aldrich), trimethyl orthoformate (TCI), camphor sulfonic acid (Sigma-Aldrich), Propanephosphonic acid anhydride (PPAA 50% w/w in ethyl acetate)(T3P), ethyl acetate HPLC grade (EtOAc)(Supelco), acetonitrile HPLC grade (ACN)(Supelco), triethylamine (TEA)(Sigma-Aldrich), hydroxylamine hydrochloride ($NH_2OH \cdot HCl$)(TCI), anhydrous sodium sulfate (Na_2SO_4)(Sigma-Aldrich), Silica gel 60A (35-70 um)(Carlo Erba),dichloromethane (DCM)(Supelco), methanol HPLC grade (MeOH)(Supelco), 2-picolinic acid (Aldrich), thionyl chloride (ThermoScientific), sodium bicarbonate ($NaHCO_3$)(Aldrich), NP-40 detergent (ThermoScientific), PalmostatinBeta (MilliporeSigma), Pierce BCA Protein Assay Kit (ThermoScientific), chloroform (Supelco), deuterated chloroform (Eurisotop), ammonium formate (Sigma-Aldrich), formic acid (Aldrich), Dulbecco's Modified Eagle Medium (DMEM)(Merk), Fetal Bovine Serum (FBS)(Gibo), Protease inhibitor cocktail (Sigma-Aldrich), phosphate buffered saline (PBS)(Sigma-Aldrich), Tris·HCl (Sigma-Aldrich).

Materials

Neuro-2a (N2a) cells were kindly provided by the Max-Planck-Institute of molecular Physiology (Dortmund, Germany) and were obtained originally from ATCC Cell lines were maintained at 37 °C in 5% CO2 in Dulbecco's Modified Eagle Medium (DMEM) with high glucose, L-glutamine and sodium bicarbonate without sodium pyruvate, supplemented with 10% fetal bovine serum and 1% Penicillin-Streptomycin.

TLC Silica gel 60 F254 aluminum sheets (Merck), cell scraper (Corning), T75 cm2 cell culture flasks with vented cap (Corning), 96 well flat bottom clear wells plates (ThermoScientific), glass chromatographic columns for flash column chromatography (Vidrefoc), UPLC mass vials (Agilent Technologies), SpeedVac (ThermoScientific), rotary evaporator (Sigama-Aldrich), centrifuge Sorvall ST1 Plus(ThermoScientific), vortex (ThermoScientific), reflux column (Sigma-Aldrich), sonicator (Sigma-Aldrich), heating plate (IKA RCT Basic).

Instruments

Bruker Ascend 400 MHz instrument (400 MHz for 1H and 101 MHz for 13C). Chemical shifts (δ) are reported in part per million (ppm) referenced to the residual solvent. Signal characterization is described using the following abbreviations: s (singlet), d (doublet), dd (doublet of doublets), t (triplet), q (quartet), p (pentuplet), m (multiplet) or br (broad signal). Spin-spin coupling constant (J) is reported in Hertz (Hz).

Mass detector for reaction monitoring: Mass detector from Waters (references: 2998, 2424 and SQ Detector 2, respectively). The instrument is equipped with a Zorbax® RR Extent C18 3.5 μm, 2.1x50 mm column from Agilent at 35 °C; flow rate: 0.7 mL/min, mobile phase: water with 0.05% of formic acid (Solvent A) and acetonitrile with 0.05% of formic acid (Solvent B); linear gradient from 5% to 100% of B over 5 minutes. The acquisition range was set to 150 – 2200 m/z and a wavelength range of 210 – 600 nm.

Software employed

Statistical tests comparing between two means have been carried out with the unpaired two-tailed t-test, between more than two means with one-way ANOVA test or Kruskal Wallis, normality of the data was tested with Shapiro-Wilk and Leven test was performed to determine equality or not of variance. Statistical differences are marked with asterisks. Statistical significance was calculated using SciPy library with Python.

For mass spectrometry analysis, MassLynx v4.2 has been used during this work.

For NMR spectra analysis and structure elucidation, MestReNova 14.2.0 was used. To represent molecules and plan the synthetic reactions both ChemDraw 21.0.0.28 and ChemDraw 23.0.1 were employed.

Finally, figures in this work were designed using BioRender, copyright-free images from the NIH (National Institutes of Health) and graphs were plotted with the use of Python libraries, specifically Matplotlib and Seaborn.

3.1 Fatty acid hydroxamate (FAH) synthesis

The synthesis of FAH was performed for FA C16:0 and C19:0 to characterize the main known fatty acid attached in S-acylation, palmitic acid and to characterize C19:0, used for the quantitative analysis of the probe.

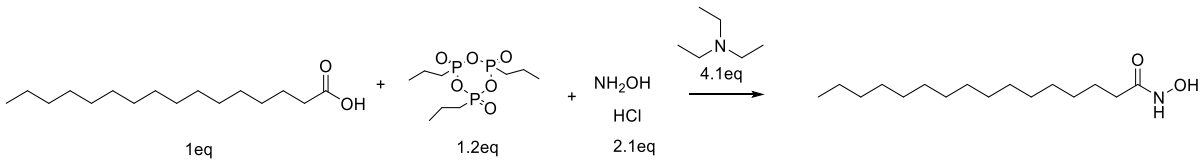

Figure 8: Synthesis of fatty acid hydroxamates from the corresponding fatty acid.

In a 10 mL round-bottom flask, 277.54 mg of PPAA (50% w/w in ethyl acetate, 520 µL, 1.2 eq) was added to 5 mL of acetonitrile (ACN). To this solution, 574.33 µL of triethylamine (TEA, 416.96 mg, 4.1 eq) was added, followed by 300 mg of C16:0 fatty acid (1.0 eq). The reaction mixture was stirred at room temperature for 30 minutes. Subsequently, 146.65 mg of hydroxylamine hydrochloride ($NH_2OH \cdot HCl$, 2.1 eq) was added, and the mixture was stirred overnight at room temperature (Figure 8).

After the overnight reaction, the progress was monitored by thin-layer chromatography (TLC) to assess completion, and mass spectrometry (MS) was used to confirm the formation of the desired product. The organic solvent was then evaporated to dryness under reduced pressure.

For purification, a liquid-liquid extraction was performed using 30 mL of ethyl acetate (EtOAc). The organic phase was washed three times with 15 mL of saturated aqueous solution (brine) in a separatory funnel. The combined organic layers were dried over anhydrous sodium sulfate, then filtered. Finally, the crude product was purified by flash column chromatography on silica gel, using a gradient of dichloromethane (DCM) and ethyl acetate (EtOAc) from 10% to 20% EtOAc, with elution monitored by TLC. Finally, the solvents were fully dried under reduced pressure, and we were left with a white powder: C16:0; 124.32mg with a 39.05% yield and C19:0; 36.79mg with a 13.47% yield.

Products were characterized via 1H NMR, 13C NMR and HR-MS for C16:0 and C19:0:

C16:0: 1H NMR (400 MHz, CDCl3) δ 2.03 (t, J = 7.5 Hz, 1H), 1.61 – 1.50 (m, 2H), 1.31 – 1.12 (m, 24H), 0.82 (td, J = 6.9, 1.8 Hz, 3H). **13C NMR** (101 MHz, CDCl3) δ 171.1, 31.99, 30.20 – 29.16 (m), 25.52, 22.76, 14.16. **HR-MS**: m/z calculated for C16H33NO2: 272.2589 [M+H]+, found: 272.2585 [M+H]+.

C19:0: 1H NMR (400 MHz, $CDCl_3$) δ 2.11 – 1.96 (m, 1H), 1.67 – 1.52 (m, 2H), 1.22 (d, *J* = 2.0 Hz, 32H), 0.85 (t, *J* = 6.7 Hz, 3H). **13C NMR** (101 MHz, CDCl3) δ 32.95, 31.90, 30.82, 29.65 (d, J = 3.7 Hz), 25.51, 22.65, 14.02. **HR-MS**: m/z calculated for C19H39NO2: 314.3059 [M+H]+, found: 314.3051 [M+H]+.

3.2 4,4-dimethoxypiperidine synthesis

For the synthesis of the derivatization agent 4,4-dimethoxypiperidine, from 4-piperidone hydrate hydrochloride, the procedure was adapted from (52).

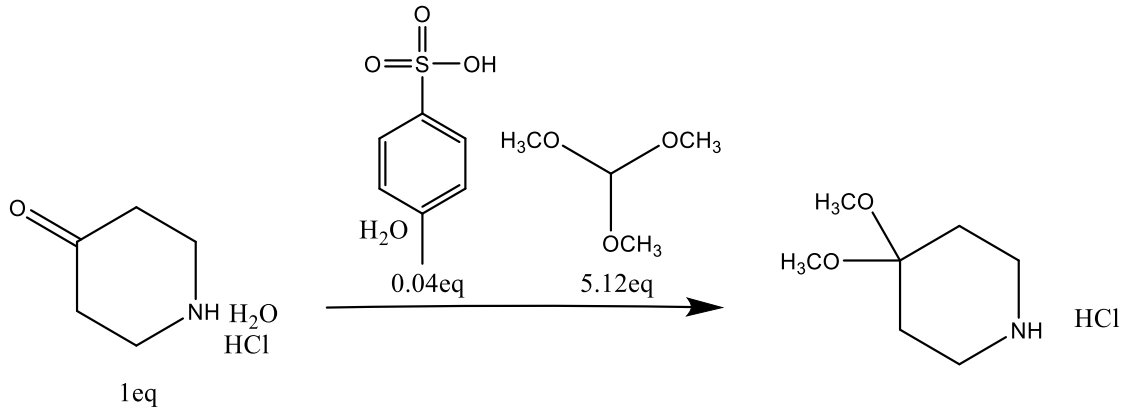

Figure 9: Synthesis of the derivatization agent 4,4-dimethoxypiperidine hydrochloride from 4-piperidone hydrate hydrochloride.

A solution of 4-piperidone 768 mg (1.0 eq, 5 mmol) was prepared in 24mL of MeOH in a 100 mL round-bottom flask. Upon complete dissolution, 38mg of p-toluenesulfonic acid monohydrate (0.04 eq, 0.2 mmol) was added, followed by the addition of 2.8 mL of trimethyl orthoformate (5.0eq, 25 mmol). The reaction mixture was stirred at room temperature for 22 hours under ambient conditions.

After completion, the reaction solvent was removed under reduced pressure. The crude residue was subjected to purification by silica gel flash column chromatography using a gradient elution system of dichloromethane (DCM) and methanol (MeOH). The elution was initiated with 3% MeOH in DCM and gradually increased to 12% MeOH, followed by a final wash with 15% MeOH to ensure complete recovery of the product. Elution progress was monitored by thin-layer chromatography (TLC).

Fractions containing the target compound were pooled and concentrated under reduced pressure. The purified product was obtained as a white solid (742.81 mg), corresponding to a

yield of 81.69%. Structural identity and purity were confirmed by nuclear magnetic resonance (NMR) spectroscopy.

1H NMR (400 MHz, CDCl3) δ 3.24 – 3.18 (m, 4H), 3.17 (s, 5H), 2.05 (t, J = 5.9 Hz, 4H). **13C NMR** (101 MHz, CDCl3) δ 96.37, 47.90, 41.49, 29.57.

3.3 Derivatization product synthesis with 4,4-dimethoxypiperidine

For the derivatization reaction of FAH with 4,4-dimethoxypiperidine, the procedure will be adapted from the one described at (50).

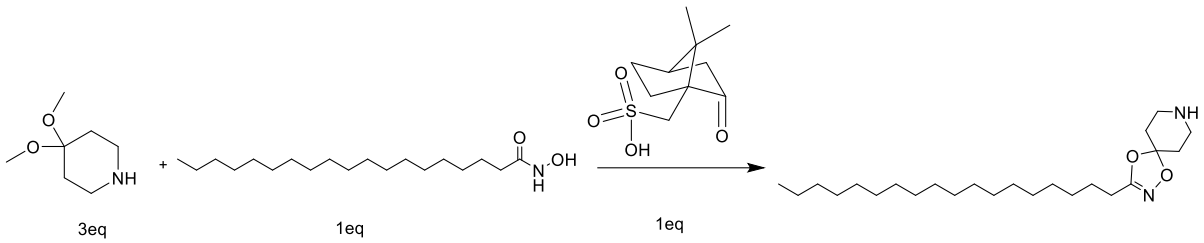

Figure 10: Derivatization reaction of fatty acid hydroxamates (FAH) via transketalization with 4,4-dimethoxypiperidine.

In a 50mL round bottom flask, 40mg (1eq, 128μmol) of FAH C16:0 was added. The flask was sealed with a rubber septum, purged with nitrogen (N_2), and maintained under an inert N_2 atmosphere throughout the reaction. Separately, a solution containing 30.80mg (1eq, 128μmol) of camphor sulfonic acid and 56mg (3eq, 192μmol) of 4,4-dimethoxypiperidine were diluted on 1mL of dry DCM. This solution was then transferred into the reaction flask via syringe, followed by an additional 2.0 mL of dry DCM to ensure complete dissolution of all reagents. The reaction mixture was stirred at room temperature under a nitrogen atmosphere for approximately 16 hours (overnight).

After the overnight reaction, the solvent was removed under reduced pressure. The crude product was analyzed by mass spectrometry (MS), which confirmed the formation of the desired compound with a molecular ion peak at: m/z 395.6422 [M+H]+. By integration of the chromatographic peak, very low amount was detected of the product and only 11% of the initial C16:0 hydroxamate had reacted. Other 30.80mg (1eq, 128μmol) of camphor sulfonic acid and 56mg (3eq, 192μmol) of 4,4-dimethoxypiperidine were added and left 8 more hours monitoring every 2 hours by MS, but no further conversion of starting material or increase in product formation was observed. Based on this observation, the reaction was deemed complete.

Despite the unsuccessful formation of the desired derivatized product, purification and characterization steps were carried out to assess the reaction outcome. The reaction mixture was subjected to a liquid–liquid extraction. The organic phase was washed twice with 4 M aqueous sodium hydroxide (NaOH) to remove any acidic by-products or unreacted starting materials. Subsequently, the organic layer was dried over anhydrous sodium sulfate (Na_2SO_4), filtered, and concentrated under reduced pressure. The resulting residue was analyzed by nuclear magnetic resonance (NMR) spectroscopy for structural characterization.

1H NMR (400 MHz, CDCl3) δ 4.05 (t, J = 6.7 Hz, 0H), 3.05 (s, 0H), 2.35 – 2.27 (m, 0H), 2.26 – 2.15 (m, 0H), 2.03 (dd, J = 13.6, 6.1 Hz, 1H), 1.91 (s, 0H), 1.70 – 1.55 (m, 1H), 1.25 (s, 16H), 0.95 – 0.80 (m, 3H). **13C NMR** (101 MHz, Chloroform-d) δ 161.75, 110.27, 42.46, 33.64, 31.81, 29.81, 29.59, 29.56, 29.53, 29.47, 29.41, 29.35, 29.08, 29.05, 28.83, 28.27, 24.96, 22.70, 14.08.

Analysis of the crude product by NMR indicated the absence of the expected derivatized compound. In particular, the characteristic signals corresponding to carbon atoms C1 and C23 (Annex 2) of the target structure were not observed in the 13C NMR spectrum.

3.4 Pyridine-2-carbonyl chloride synthesis

The synthesis of the derivatization agent was performed from 2-Picolinic acid following the classical transformation of carboxylic acids to the corresponding acyl chlorides with thionyl chloride (57).

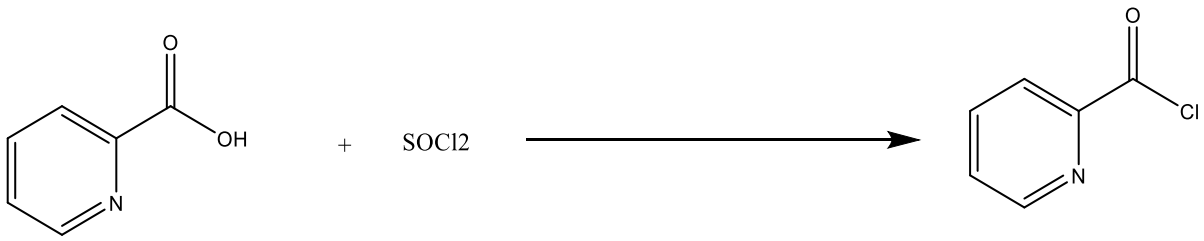

Figure 11: Synthesis of derivatization reagent pyridine-2-carbonyl chloride from 2-picolinic acid.

To a 100 mL round-bottom flask, 250 mg of 2-picolinic acid were added. The flask was placed in an oil bath and heated to 50 °C under continuous stirring. Thionyl chloride (4 mL) was then added dropwise until complete dissolution of the starting material. The reaction mixture was maintained under reflux for 2 hours, equipped with a gas release trap to safely vent the gaseous by-products (Figure 11). After the 2h of reaction, the thionyl chloride was dried under reduced

pressure and we were left with a green powder; 285mg with a 99.1% yield. Product was characterized via 1H NMR and 13C NMR.

1H NMR (400 MHz, CDCl3) δ 8.88 – 8.82 (m, 1H), 8.15 (dt, J = 7.9, 1.1 Hz, 1H), 7.93 (td, J = 7.7, 1.7 Hz, 1H), 7.61 (ddd, J = 7.6, 4.7, 1.2 Hz, 1H). **13C NMR** (101 MHz, $CDCl_3$) δ 159.57, 148.24, 146.59, 138.66, 127.98, 124.17.

3.5 Derivatization product synthesis with pyridine-2-carbonyl chloride

For the derivatization reaction of FAH with pyridine-2-carbonyl chloride, the procedure will be adapted from the one described at (58).

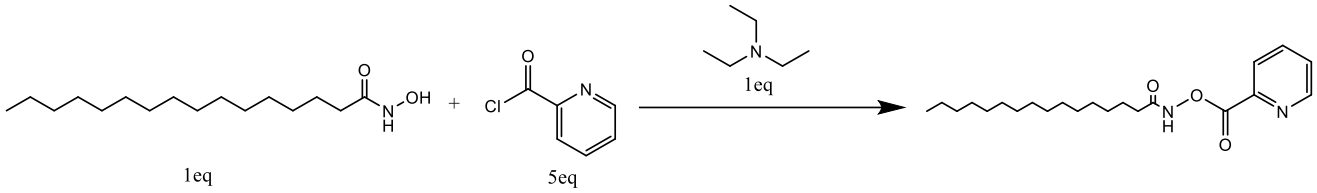

Figure 12: Derivatization reaction of fatty acid hydroxamates (FAH) via acylation with pyridine-2-carbonyl chloride

A total of 260 mg (5 eq, 1.84 mmol) of pyridine-2-carbonyl chloride was added to a 100 mL round-bottom flask equipped with a magnetic stir bar. The flask was sealed with a rubber septum, purged with nitrogen gas via syringe, and connected to a nitrogen balloon to maintain an inert atmosphere. The flask was then placed in an ice bath (0 °C).

In a separate vial, (1 eq, 368.4 µmol) of the corresponding fatty acid hydroxamate (FAH) was dissolved in 2 mL of dry dichloromethane (DCM). To this solution, 51 µL (1 eq, 368.4 µmol) of triethylamine (TEA) was added. The resulting mixture was transferred into the reaction flask via syringe under nitrogen. An additional 2 mL of dry DCM was then added to the flask. The reaction mixture was stirred overnight at 0 °C under a nitrogen atmosphere (Figure 12).

After the overnight reaction, the solvent was removed under reduced pressure. The crude product was analyzed by mass spectrometry (MS), which confirmed the formation of the desired compound with a molecular ion peak at **C16:0**: m/z 377.2804 [M+H]+ and **C19:0**: m/z 419.3274 [M+H]+. Integration of the chromatographic peak area indicated that 92.81% of the initial FAH had reacted.

Due to low solubility and the presence of excess unreacted pyridine-2-carbonyl chloride, nuclear magnetic resonance (NMR) analysis required a purification step. A liquid-liquid

extraction was performed by dissolving the crude product in 10 mL of dichloromethane (DCM) and washing the organic phase twice with 10 mL of a basic aqueous sodium bicarbonate ($NaHCO_3$) solution. The organic phase was dried over anhydrous sodium sulfate (Na_2SO_4), filtered and the solvent was removed under reduced pressure. This step served to hydrolyze the excess acid chloride back into picolinic acid and HCl, which are more water-soluble under basic conditions, thereby effectively removing them from the organic layer. The purified organic phase was then prepared for NMR analysis.

1H NMR (400 MHz, CDCl3) δ 8.25 – 8.11 (m, 1H), 7.89 (tdd, J = 7.8, 3.6, 1.8 Hz, 1H), 7.61 – 7.50 (m, 1H), 2.34 (t, J = 7.6 Hz, 1H), 1.71 (p, J = 7.6 Hz, 2H), 1.25 (s, 25H), 0.87 (t, J = 6.7 Hz, 3H). **13C NMR** (101 MHz, CDCl3) δ 171.29, 166.01, 163.42, 162.45, 151.37, 150.38, 150.26, 148.85, 145.65, 145.32, 137.46, 137.32, 137.06, 128.08, 128.01, 126.40, 126.28, 126.10, 124.21, 77.36, 45.74, 36.67, 33.03, 32.06, 29.83, 29.81, 29.78, 29.74, 29.58, 29.49, 29.47, 29.42, 29.27, 29.11, 25.26, 24.31, 22.82, 14.25, 8.76, 1.15.

Further purification was performed using flash column chromatography on silica gel. The product was eluted with a gradient of dichloromethane (DCM) and methanol (MeOH), starting from 1.5% to 10% MeOH, followed by a final wash with 15% MeOH to ensure complete elution. The separation was monitored by thin-layer chromatography (TLC). After collecting and combining the fractions containing the desired compound, solvents were removed under reduced pressure. The resulting product was obtained as a white powder, with a final recovery of 80 mg, corresponding to a yield of 57.67%.

Final NMR was performed to assess the final purity of the product.

1H NMR (400 MHz, CDCl3) δ 8.76 (dd, J = 12.0, 4.4 Hz, 1H), 8.23 – 8.11 (m, 1H), 7.88 (qd, J = 7.8, 1.7 Hz, 1H), 7.55 (ddd, J = 7.7, 4.8, 1.2 Hz, 1H), 2.34 (t, J = 7.5 Hz, 2H), 1.71 (p, J = 7.4 Hz, 2H), 1.43 – 1.14 (m, 26H), 0.87 (t, J = 6.8 Hz, 3H). **13C NMR** (101 MHz, CDCl3) δ 163.47, 150.28, 145.55, 137.48, 128.04, 126.12, 77.36, 53.56, 33.15, 32.05, 29.83, 29.81, 29.78, 29.74, 29.58, 29.49, 29.43, 29.28, 25.25, 22.82, 14.25.

As shown in Annex 3, the final derivatized product exhibits high purity, as evidenced by the absence of significant impurities in the chromatographic profile, in the integrals of the peaks and the well-defined mass corresponding to the expected product.

3.6 Derivatization of C16:0 and C19:0 FAH: Pre- and Post-Reaction Analysis

To directly evaluate the signal enhancement resulting from derivatization in HPLC-HRMS, 10 µM solutions of the pure synthetic standards were prepared. These included C16:0 FAH, C16:0 derivatized, C19:0 FAH, and C19:0 derivatized. Each compound was dissolved in methanol (MeOH), and all samples were prepared in duplicate. A volume of 300 µL of each solution was transferred into mass spectrometry vials for analysis.

3.7 Calibration curve, LOD and LOQ of C16:0 derivatization product

With the aim of checking the linearity of the signal on the HPLC-HRMS and the limit of detection (LOD) and limit of quantification (LOQ) of C16:0 derivatized, a 1 mM stock solution of the C16:0 derivatized product was prepared in HPLC-grade methanol. From this solution, a series of ten 1:2 serial dilutions followed by two additional 1:100 dilutions were performed, resulting in a final concentration range from 500 µM to 97.6 pM. Each dilution was prepared in triplicate, and 300 µL of each solution was transferred into mass spectrometry vials for HPLC-HRMS analysis.

3.8 One-pot reaction

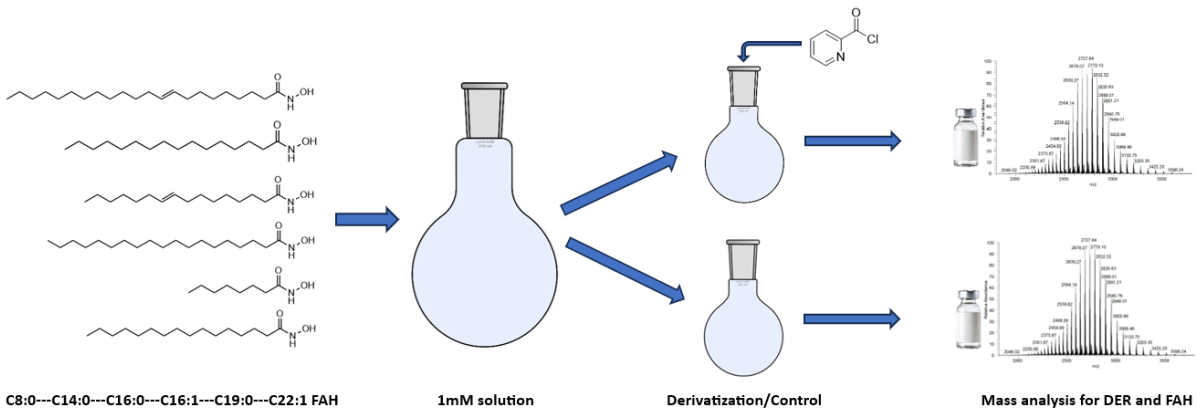

Figure 13: Workflow for the one-pot reaction methodology and analysis.

To assess the enhancement of MS detection of FAH under conditions simulating real sample complexity, a mixture containing various FAH species, including long- and short-chain, saturated and unsaturated derivatives was subjected to derivatization. Following the reaction,

only a basic workup was performed, and the crude mixture was directly injected into the HPLC-HRMS to evaluate the reactivity and detectability of the different FAH types.

Stock solutions (1 mM in methanol) of six different fatty acid hydroxamates (FAHs): C8:0, C14:0, C16:0, C16:1, C19:0, and C22:1 (With the exception of C16:0 and C19:0, all other fatty acid hydroxamates (FAHs) had been previously synthesized by the group) were prepared. From each stock, 3.7 mL (corresponding to 3.70 µmol) was combined in a 10 mL round-bottom flask. The resulting mixture was then split equally into two separate 10 mL round-bottom flasks, and methanol was removed under reduced pressure.

To one of the flasks (derivatized sample), 7.86 mg of pyridine-2-carbonyl chloride (5 equivalents, 55.5 µmol) and 15.5 µL of a 1:10 dilution of triethylamine (TEA) (1 equivalent, 11.1 µmol) were added in 500 µL of dry dichloromethane (DCM). The reaction was stirred in an ice bath at 0 °C overnight.

The second flask (non-derivatized control) was treated with 500 µL of dry DCM and left to stir under the same conditions (ice bath, overnight) to maintain consistent handling across both samples.

After the overnight reaction, we did the work-up consisting in the already mentioned liquid to liquid extraction. 10mL of DCM was added in both flasks and each flask was then washed two times on an extraction funnel with 10mL of a basic aqueous solution ($NaHCO_3$). The organic phases were dried over anhydrous sodium sulfate (Na_2SO_4), filtered and the solvent was removed under reduced pressure.

Finally, 1.10 mL of HPLC-grade methanol was added to each flask containing the dried products to prepare 10 mM stock solutions. These were subsequently diluted 1:100 to obtain 100 µM solutions, one containing the non-derivatized FAH mixture and the other its corresponding derivatized form. Triplicates of each solution were prepared by transferring 300 µL into individual mass spectrometry vials for analysis.

3.9 Analysis of the S-Acylome in N2a Cells: Comparison of FAH and Derivatized Probes

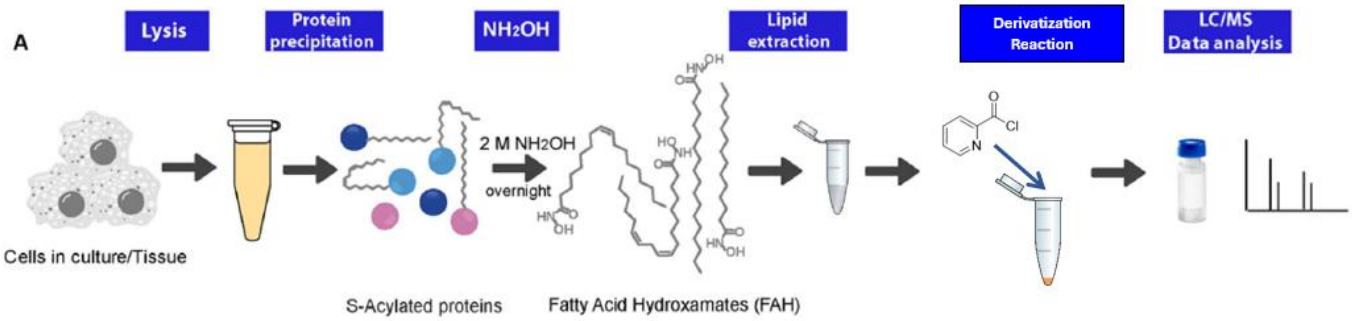

Figure 14: New derivatization procedure for the enhanced probe for qualitative and quantitative analysis of the S-acylation on cell lysates.

This procedure is adapted from the previously described probe presented by this research group (21).

N2a cells starting from an 18 pass are seeded in 4 T75 flasks and left to grow to confluence (90%). The cell media is aspirated, and the cells are washed with phosphate-buffered saline (PBS), then, collected using cell scrapers in 1mL per flask of media. The cell suspension is centrifuged (400 g, 3 min, rt), the supernatant is removed, and the cell pellet is washed with PBS (2 mL, 400 g, 3 min, rt) twice.

The cell pellet is then resuspended in a $10x10^6$ cells/mL ratio with lysis buffer (50 mM Tris·HCl, 150 mM NaCl, pH 7.2) containing protease inhibitors, 1% of NP-40, and 10 µM of PalmB (inhibition of thioesterases). The cells are lysed by sonication at 0 °C (10 cycles, 5 seconds sonication followed by 5 seconds resting period, intensity at 50%). After clarification (3000 g, 5 min, rt) the cell lysates are transferred into 15 mL plastic Falcon tubes and the protein is precipitated by the use of organic solvents (59). Briefly, the method consists of subsequently adding: 4 volumes (V) of methanol, 1.5 V of chloroform and 3 V of H2Odd to the lysates. After each solvent addition a vortex mixer is used to ensure proper homogenization. After centrifugation (6000 g, 20 min, rt) the protein pellet appears in the interphase. The upper layer (aqueous phase) is removed, and 3 additional V of MeOH are added and the samples centrifuged again (6000 g, 10 min, rt) to remove the remaining organic phase. The pellet is dried under a stream of nitrogen and resuspended in 1mL lysis buffer (50 mM Tris·HCl, 150 mM NaCl, pH 7.2) in the same volume and mixed thoroughly with a micropipette.

An aliquot (20 µL of the dissolved proteome and 180 µL of H2Odd) is used to quantify the total amount of protein by BCA.

A calibration curve of protein is prepared according to the manufacturer instructions provided in the PierceTM BCA Protein Assay Kit. In a clear-bottom 96-well plate, 10 µL of each protein concentration are added to each well. Three replicates of the calibration curve are prepared in each measurement. A 1:10 dilution of the sample (cell lysate or proteome) in H2OmiliQ is prepared and 10 µL are also introduced in a well three times. Then, following the kit instructions, reagent A and B are mixed in a 50:1 proportion and 200 µL of this mixture are added into each well containing analyte. The plate is left covered for 30 min at 37 ºC. Afterwards, the protein is quantified in a BioTek Synergy H1 microplate reader at 562 nm using the Gen5 software.

Once quantified, the proteome is split into 1200 µg of protein per portion in 1.5 mL Eppendorf tubes. In this case we divided into 6 portions. Then, an equal volume of buffer (for the blanks) or a 4 M solution of hydroxylamine in buffer (previously adjusted to pH 7.4) is added to the samples and left overnight with end-over-end rotation at room temperature.

The next day, 100 pmol of the internal standard (C19:0 FAH) is added into each sample and the solution is transferred into glass vials. Lipid extraction is performed (60) by the successive addition of 3.75 V of a 1:2 (v/v) solution of chloroform and methanol, 1.25 V of chloroform and 1.25 V of H2Odd. A vortex mixer is also used. After 1–2 minutes, two distinct phases formed in the samples. The organic phase (lower layer) was carefully transferred into new Eppendorf tubes, and the solvent was evaporated under a gentle nitrogen stream.

Each dried sample was then resuspended in 400 µL of dichloromethane (DCM) and split equally into two separate tubes: one designated as a control (non-derivatized) and the other for derivatization.

To the control samples, an additional 200 µL of DCM was added to maintain the same volume. For the derivatization samples, the following were added: 148.63 µL (5 equivalents, 1.05 µmol) of a 1 mg/mL solution of pyridine-2-carbonyl chloride in DCM, 29.61 µL (1 equivalent, 0.21 µmol) of a 1:1000 dilution of triethylamine (TEA) and 21.76 µL of DCM to bring the final volume to 400 µL.

These reagent volumes were calculated based on previous experiments performed within this research group, which established that for every 1 mg of protein, approximately 70,000 pmol of FAH are present. Given that each sample contained approximately 600 µg of protein, this corresponds to an estimated 0.042 µmol of FAH per sample. A 5-fold molar excess of

derivatizing agent was applied to ensure complete reaction beyond the theoretical stoichiometric equivalents, setting 1 equivalent at 0.21 µmol.

The samples were incubated overnight at 4 °C with end-over-end rotation in a refrigerated chamber to allow the derivatization reaction to proceed. Following the reaction, each sample was transferred into a mass spectrometry vial and the solvent was removed using a SpeedVac concentrator. The dried samples were then stored at –20 °C until analysis. Immediately prior to HPLC-HRMS injection, the samples were resuspended in 300 µL of HPLC-grade methanol.

3.10 HPLC-HRMS lipidomic analysis

For the analysis an ESI Quadrupol-Time-of-Flight (Q-TOF) Cyclic IMS controlled with Waters Micromass MassLynx v 4.2 SCN 016 Software, and equipped with an AcquityTM Premier BEH C18 column (1.7 µm particle size, 50 mm × 2.1 mm, Waters) with a VanGuardTM FIT pre-column was used. Samples were also injected through a cooled autosampler at 10 °C. A flow rate of 0.3 mL/min was applied, the column was thermostated at 30 °C and an injection volume of 5 µL. The acquisition range of the TOF detector was m/z 50 to 1.200, the capillary voltage was set to 3.0 kV, the desolvation temperature was 250 °C and the desolvation gas flow rate was 800 liters/h.

For proper separation of the detected hydroxamates and its derivatives, the mobile phase was 2 mM ammonium formate and 0.2% formic acid in water (Solvent A) and 1 mM ammonium formate and 0.2% formic acid in methanol (Solvent B). Gradient elution started at 65% Solvent B, increased to 99% over 15 min., held for 2 min., and then returned to 65% Solvent A over 3 min as depicted in the following table:

Table 2: LC conditions for the analysis of FAH and derivates employed in the LC-HRMS.

Time (min)	Flow (mL/min)	%A	%B	Curve
Initial	0.3	35	65	6
2	0.3	35	65	6
10	0.3	10	90	6
15	0.3	1	99	6
17	0.3	1	99	6
20	0.3	35	65	6
22	0.3	35	65	6

4. RESULTS

All results presented in this section correspond to derivatization reactions performed using pyridine-2-carbonyl chloride. As described in the methodology section, the use of 4,4-dimethoxypiperidine as a derivatization agent was discontinued at an early stage due to its low reactivity, the formation of numerous by-products (Annex 1), and the inability to isolate or characterize the desired product.

4.1 C16:0 and C19:0 derivatized product analysis

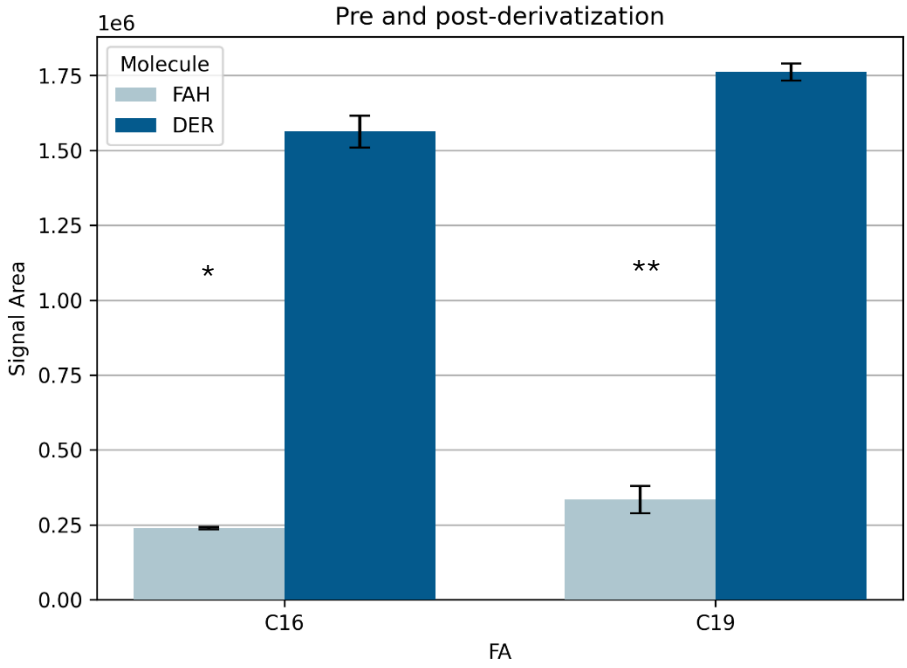

Figure 15: Signal area of the pure products C16:0 FAH, C16:0 DER, C19:0 FAH and C19:0 DER. *'**$p < 0.005$. n=3.

As shown in Figure 15, the derivatized fatty acid hydroxamates (FAHs) exhibit a notably enhanced signal intensity in the HPLC-HRMS analysis compared to their underivatized counterparts. When injected at the same concentration (10 µM) under identical analytical conditions. This result demonstrates the effectiveness of the derivatization strategy in increasing the analytical response of FAHs.

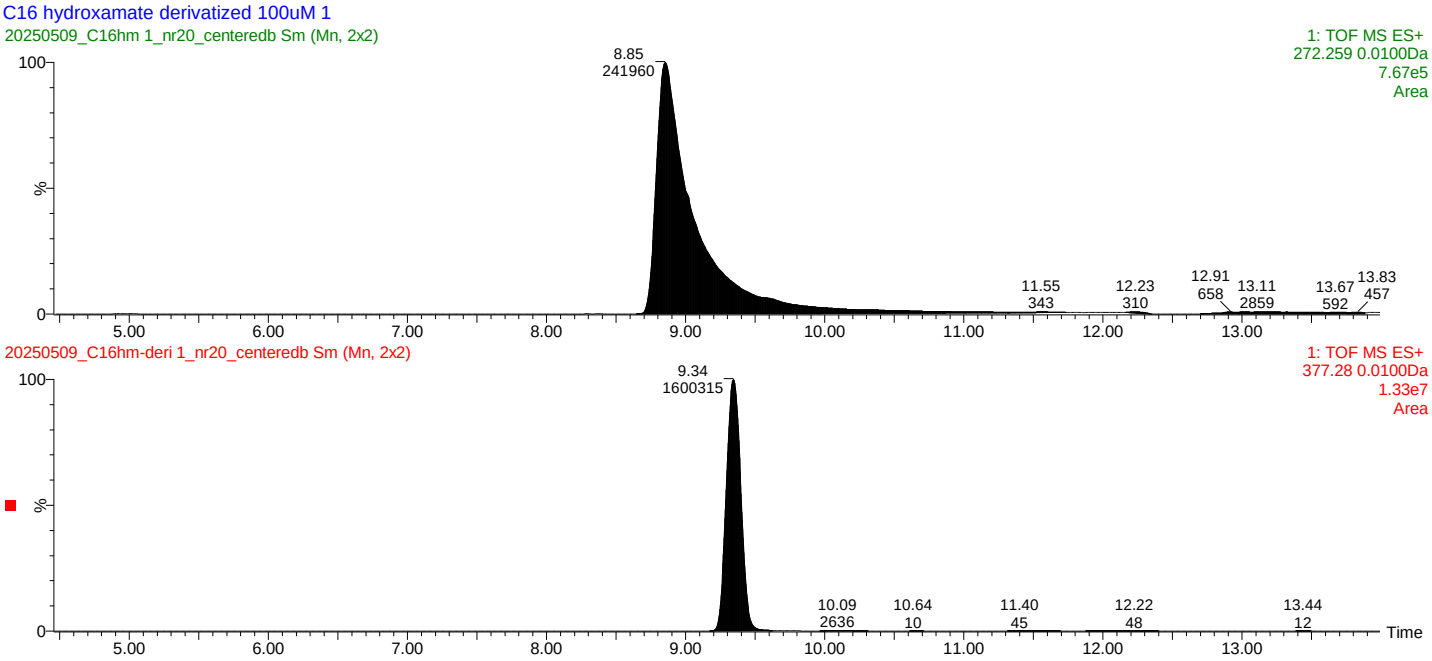

Figure 16: Chromatographic signal area of C16:0 FAH (green) compared to chromatographic signal area of C16:0 FAH after derivatization with pyridine-2-carbonyl chloride (red).

Moreover, as illustrated in Figure 16, the chromatographic profile of the derivatized product exhibits a sharper, more symmetrical, and well-resolved peak in comparison to the underivatized FAH. In contrast, the FAH signal displays a broadened, tailing peak, which is indicative of metal ion complexation, consistent with the known chelating properties of hydroxamate groups. This tailing effect can compromise the accuracy and reproducibility of quantitative analysis. The improved peak shape observed for the derivatized product not only facilitates more reliable integration but also underscores the analytical advantage of derivatization in mitigating metal induced peak distortion, ultimately leading to more accurate and reproducible quantification.

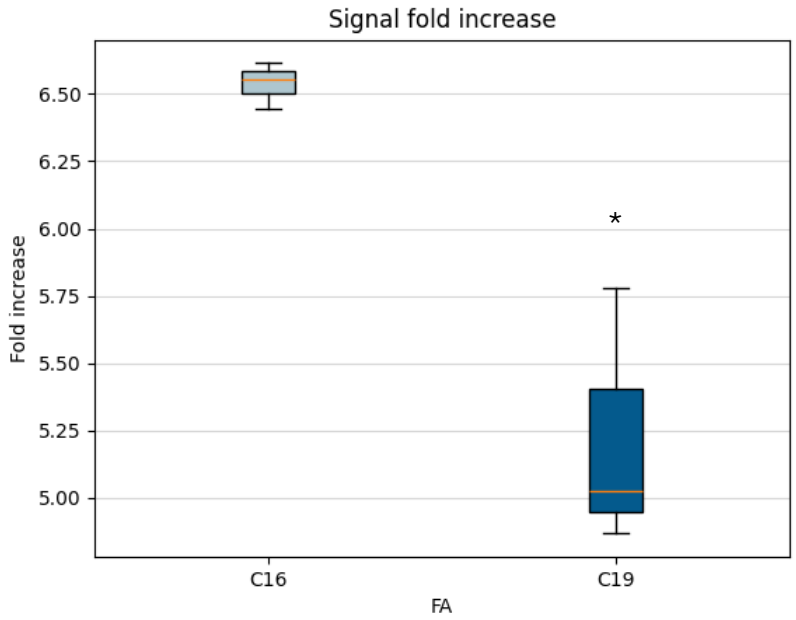

Figure 17: Fold increase in the signal area. Before derivatization and after C16:0 and C19:0 FAH. * p = 0.022.

The fold increase in chromatographic signal area was calculated as the ratio of the area of the derivatized product and the FAH. As shown in Figure 17, the fold increases were 6.53 for C16 and 5.33 for C19, with a statistically significant difference between them. Ideally, all fatty acids should exhibit a similar fold increase to ensure quantitative reliability of the analysis. The observed discrepancy may be attributed to lower purity achieved during the purification of the derivatized form of C19 what may have a slight effect on the final stock concentrations performed. Additional replicates will be prepared with new stock solutions to investigate this possibility.

4.2 Linearity of the signal, LOD and LOQ

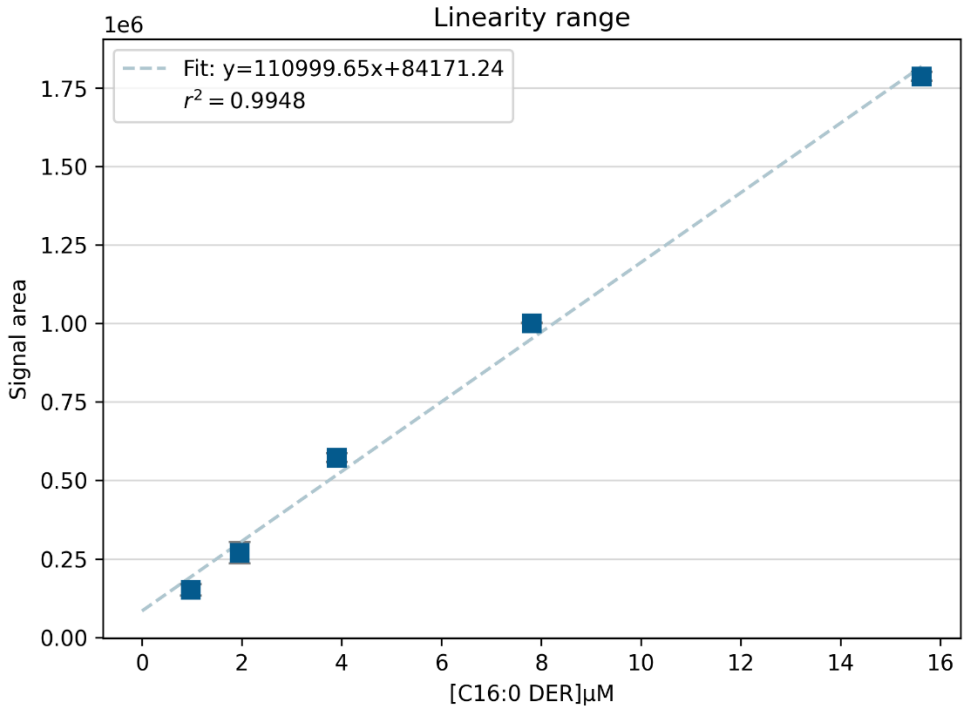

Figure 18: Range concentration of derivatized product C16:0 with linear signal over HPLC-HRMS

The linearity of the analytical response, as well as the limit of detection (LOD) and limit of quantification (LOQ) for the C16 derivatized product, were subsequently evaluated using the signal-to-noise (S/N) ratio method, which is a widely accepted approach in mass spectrometry-based quantification. According to standard analytical guidelines, a S/N ratio of 3 is typically used to estimate the LOD, representing the lowest concentration at which the analyte can be reliably distinguished from the baseline noise. Conversely, a S/N ratio of 10 is employed to define the LOQ, representing the lowest concentration at which the analyte can be quantified with acceptable precision and accuracy.

To establish the dynamic working range of the method, a calibration curve was constructed using a series of known concentrations of the C16 derivatized product. The working range was defined as the concentration interval extending from the LOQ to the maximum concentration used in the calibration, with a correlation coefficient (r^2) maintained above 0.98 to ensure acceptable linearity and robustness of the response (Figure 18). Within this range, the mass spectrometry (MS) response was found to be linear up to 15.625 mM, confirming the suitability of the method for quantitative applications.

Based on the S/N analysis, the LOD for the C16 derivative was determined to be 9.76 nM, corresponding to approximately 48.85 picomoles of analyte injected onto the column. The LOQ was established at 0.976 mM, equivalent to 4.88 nanomoles of injected product. These sensitivity parameters demonstrate the method's capacity to detect and accurately quantify the derivatized C16 species over a broad concentration range, supporting its applicability for detailed quantitative lipidomic or fatty acid profiling studies.

4.3 One-pot reaction

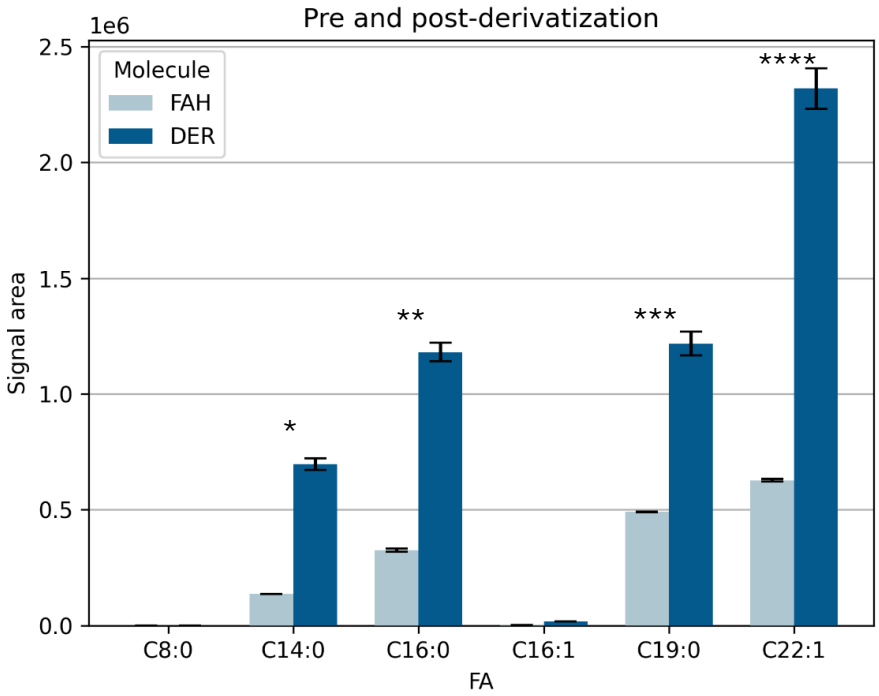

Figure 19: Signal area of FAH; C8:0, C14:0, C16:0, C16:1, C19:0 and C22:1. Before and after derivatization. *, **, ***, ****p < 0.001.

Next, the effect of the derivatization reaction on FAH of different lengths was investigated. As observed in Figure 19, the FAH derived from C14:0, C16:0, C19:0, and C22:1 exhibit a clear and significant increase in signal area following derivatization, compared to their corresponding non-derivatized FAH forms. This enhancement highlights the effectiveness of the derivatization strategy in improving MS detection. However, it is also evident that the initial signal intensities of the FAHs prior to derivatization vary considerably across the different species. This variability may reflect differences in the purity or concentration of the starting FAH materials, which could have influenced the observed signal areas independently of the

derivatization process. To address this, quantitative NMR with an internal standard should have been used to verify the purity of each FAH before derivatization. The almost inexistence of C8:0 and C16:1 may also be dure to this problem.

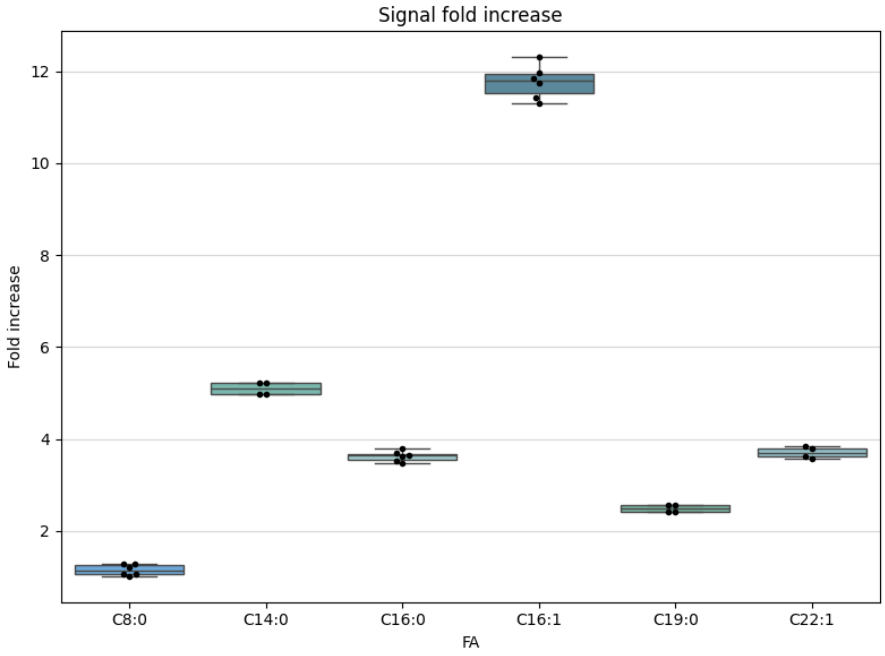

Figure 20: Fold increase in the signal area after derivatization of C8:0, C14:0, C16:0, C16:1, C19:0 and C22:1.

When examining the fold increase in signal intensity following derivatization (Figure 20) it is evident that fatty acids C14:0, C16:0, C19:0, and C22:1 display enhancements ranging approximately from 2 to 5-fold. While all compounds show statistically significant differences in fold increase (except between C16:0 and C19:0) this variation raises important considerations. Theoretically, the fold increase should not be influenced by differences in sample purity, as it is derived from the ratio of signal intensities before and after derivatization. Nevertheless, the observed disparities suggest that other factors may be contributing to this variability. These may include differences in reaction kinetics or derivatization efficiency across the various FAH species, changes in solubility or inconsistencies in ionization or detection sensitivity in the HRMS analysis. Such factors could differentially impact the overall analytical response and should be taken into account when interpreting quantitative comparisons across derivatized FAHs. Lastly, the fold increase for C8:0 was approximately 1, as its signal remained near the detection limit both before and after derivatization, indicating the almost nonexistence of the product. In contrast, C16:1 exhibited a notably high fold increase of 11.7. This outlier is likely attributable to an initially low concentration of starting

material, leading to an underestimated pre-derivatization signal and, consequently, an inflated fold change.

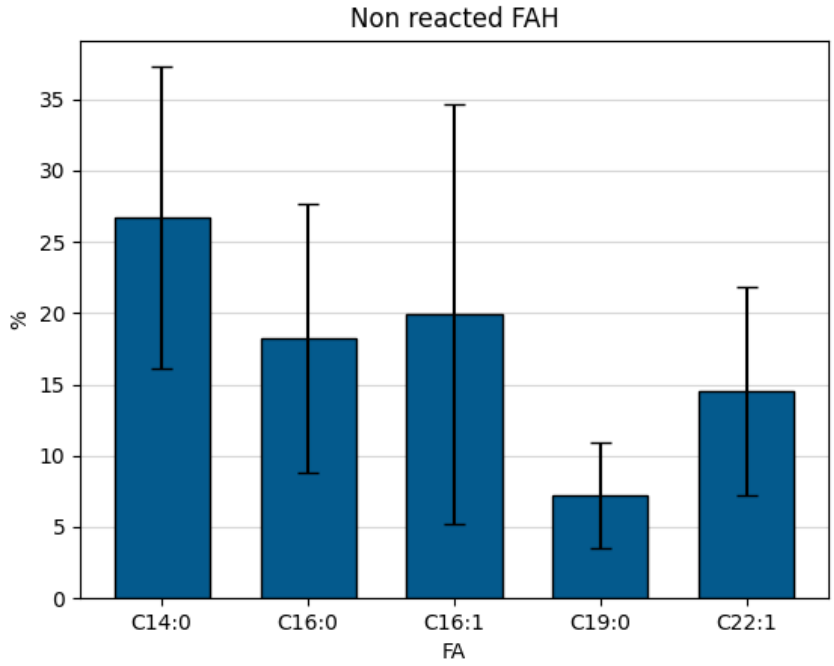

Figure 21: Percentage of unreacted FAH after derivatization of, C8:0, C14:0, C16:0, C16:1, C19:0 and C22:1.

The percentage of unreacted FAH remaining after the derivatization reaction was also assessed in order to evaluate the reaction efficiency and explore potential differences in reaction kinetics among the FAH species. As shown in Figure 21, the quantification of unreacted FAH was associated with substantial variability, primarily due to the very low residual amounts of FAH detected post-reaction. This limited quantity hindered accurate and reliable measurement, thereby compromising the ability to draw meaningful conclusions regarding incomplete derivatization. As a result, no statistically significant differences were observed between the FAH species, and the data does not support a clear interpretation of kinetic differences under the current experimental conditions. However, with this information, in hand, longer reaction times or different reaction conditions should be explored to ensure a quantitative derivatization reaction of FAH.

4.4 Analysis of the S-Acylome in N2a Cells

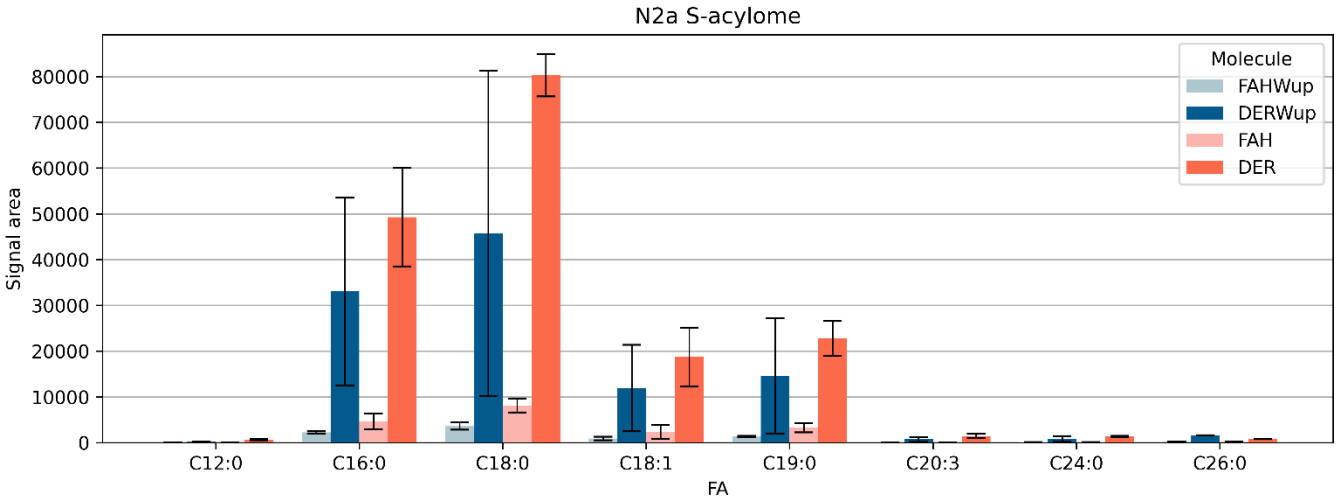

Figure 22: The S-acylome profile of different FA, pre- and post-derivatization and with or without liquid-liquid extraction (Wup).

After these preliminary studies performed using synthesized and purified FAH, it was decided to explore the suitability of the reaction using the cell proteome. With this aim, the cells were lysed, the proteome was precipitated and treated with NH2OH overnight to generate the corresponding FAH that when then extracted. These extracted FAH were then treated overnight with the derivatization reagent. Some samples underwent liquid-liquid extraction to remove the derivatization agent from the sampler. These were then compared to non-extracted samples to assess whether the presence of the derivatization agent interfered with the HPLC-HRMS analysis.

To comprehensively profile the S-acylome, a diverse panel of FAH was selected to be analysed, encompassing a range of carbon chain lengths as well as degrees of saturation, analysis can be seen in Annex 4. As illustrated in Figure 22, all analyzed FAH exhibited a marked increase in signal intensity following the derivatization step. Notably, the fatty acid 20:3, which was undetectable prior to derivatization likely due to its low endogenous abundance and the limited sensitivity of the FAH form became readily detectable following the derivatization process confirming the effectiveness of the chemical modification in enhancing FA detectability.

Furthermore, a comparison between samples subjected to a liquid-liquid extraction ("work-up") and those processed without this step revealed notable differences. Specifically, non-extracted samples consistently displayed higher signal intensities, suggesting that a significant portion of FAs may be lost during the extraction procedure. In addition, samples that underwent the work-up process exhibited greater signal variability, which may reflect procedural

inconsistencies inherent in the extraction step when applied to small-scale samples such as cell lysates. This variability underscores the challenges of reproducibility in such workflows.

Collectively, these observations indicate that omitting the liquid-liquid extraction step yields more robust and consistent results. Thus, for the analysis of S-acylated proteins in cell lysates, direct derivatization without subsequent extraction appears to be the most reliable and efficient approach.

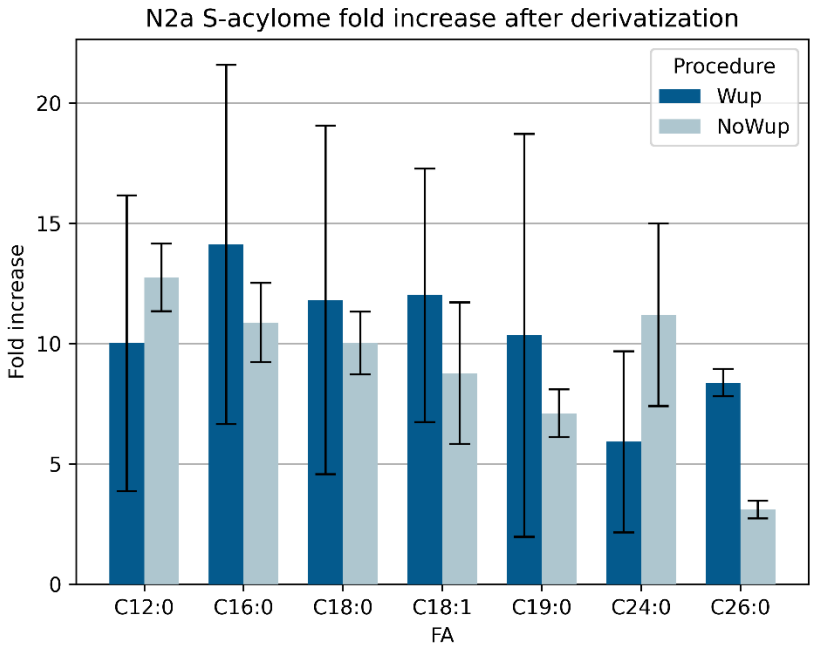

Figure 23: Fold increase of the signal area after derivatization reaction on N2a cell lysate.

Lastly, the fold increase in signal was calculated for both the samples subjected to the work-up procedure and those that were not. As illustrated in Figure 23, unlike what was observed with the one-pot reaction, the variation in fold increase across different fatty acids is markedly reduced in this setup. In fact, no statistically significant differences were observed between the FAH, and in most of the cases the enhance in the signal response area was around 10, with the exception of C12:0 and C26:0 in the non-work-up group ($p < 0.033$).

However, consistent with previous observations, samples that underwent the liquid-liquid extraction exhibited substantially higher variability. This increased variance is likely due to the inherent difficulty in achieving reproducible extraction when working with very small sample volumes, which can lead to inconsistent recovery of analytes.

Importantly, the relative consistency of the fold increase across the fatty acid panel serves as a positive indicator of the robustness of the derivatization reaction. This consistency suggests

that the chemical modification preserves the quantifiable characteristics of the hydroxylamine probe, thereby supporting the reliability of this approach for comparative analysis of fatty acylation profiles.

5. CONCLUSIONS

In summary, based on the results presented here and prior studies, it can be concluded that:

- Acylation with pyridine-2-carbonyl chloride was successfully validated as an effective derivatization method for fatty acid hydroxamates (FAHs), as the synthesis of the derivatized product was successful and detection was significantly enhanced. In contrast, transketalization with 4,4-dimethoxypiperidine exhibited low reaction yields and was subsequently discarded.

- The derivatization of FAH retained quantitative capabilities and improved analytical sensitivity, though some inconsistencies in response between fatty acid species were noted.

- The derivatized probe was successfully applied to characterize the S-acylome of N2a cells, increasing the signal and accuracy of detection of different fatty acids demonstrating its potential for biological and disease-related studies.

- This preliminary approach holds promising to enhance the mass-based detection of hydroxamates, although the reactions conditions need to be optimized to ensure a quantitative reaction and explore if the derivatization reaction takes place with similar efficiencies for both FAH of short and long chains, as well as bearing one or multiple unsaturations.

6. DISCUSSION

The primary objective of this study was to improve the detection of fatty acid hydroxamates (FAH) through a derivatization step to enhance the ionization properties of the molecule, thereby enhancing the qualitative and quantitative analysis of S-acylated lipids in biological samples, particularly in N2a cell lines. This analytical strategy was developed in response to the limitations of the hydroxylamine HPLC-HRMS-based detection probe of the S-acylome (23)(21), which include low ionization efficiency, chromatographic distortions due to chelating properties of FAH and poor sensitivity toward low-abundance species.

Until today, numerous derivatization strategies have been developed to improve the mass spectrometric detection of fatty acids. One of the most well-known examples is the work by Wen-Chu Yang and colleagues, who employed 2-bromo-1-methylpyridinium iodide and 3-carbinol-1-methylpyridinium iodide to derivatize free fatty acids. This reaction forms 3-acyloxymethyl-1-methylpyridinium iodide (AMMP), a highly ionizable compound that enhances electrospray ionization efficiency, leading to up to a 2500-fold increase in detection sensitivity compared to the non-derivatized form of the fatty acid. Other strategies have used quaternary ammonium salts, pyridinium moieties, or tertiary amine-containing reagents to similar effect, often targeting the carboxylic acid group common to free fatty acids (48).

However, these strategies are typically optimized for the analysis of free, unbound fatty acids. They do not address the specific analytical challenges posed by fatty acid hydroxamates (FAH), which are the key analytes generated by hydroxylamine-mediated cleavage of thioester bonds in S-acylated proteins. Unlike free fatty acids, FAHs contain a hydroxamic acid group instead of a carboxylic acid, resulting in markedly different chemical properties.

Consequently, derivatization strategies designed for carboxylic acids are often ineffective or suboptimal for FAHs. In our study, we aimed to overcome these limitations by exploring derivatization reactions specifically suited to the chemical nature of hydroxamic acids. Among the tested approaches, we focused on the acylation of the hydroxamic acid group using pyridine-2-carbonyl chloride. This reagent introduces a pyridyl moiety, well known for its favorable ionization characteristics under positive ESI conditions (49), onto the hydroxamate, producing a stable O-acylhydroxamate derivative.

Unlike previously described methods that target the carboxylic acid group our derivatization approach for hydroxamic acid offers several advantages:

High Efficiency and Yield: The derivatization reaction proceeded with yields consistently above 90% under mild conditions (0 °C, overnight), which is crucial for preserving analyte integrity, maintaining the quantitative properties of the probe and achieving reproducible results in biological samples.

Improved Chromatographic Behavior: The derivatized FAHs exhibited sharper, more symmetrical peaks with significantly reduced tailing, a clear benefit over the native hydroxamate probe, which suffered from metal-induced chromatographic distortions (45).

Increased Sensitivity: When analyzed by HPLC-HRMS, the derivatized C16:0 and C19:0 FAHs showed signal intensities 5.3- to 6.5-fold higher than their underivatized counterparts at the same concentrations. This enhancement is less dramatic than the 2500-fold increase reported for AMMP-derivatized carboxylic acids, but it is both statistically significant and analytically meaningful, especially considering the limited ionization potential of hydroxamic acids.

Retention of Quantitative Features: Importantly, the derivatization did not compromise the method's quantifiability. The derivatized products retained a linear response across a broad concentration range, with a correlation coefficient (R^2) greater than 0.98, and demonstrated low limits of detection (9.76 nM for C16:0 derivative), making the approach suitable for both qualitative profiling and quantitative comparison of FAH species.

Despite the numerous positive outcomes and achievements associated with this method, certain limitations remain that hinder its full standardization. One significant drawback is the observed variability in signal enhancement across different FAH (fatty acid hydroxamate) species.

Several factors could contribute to this phenomenon, with one plausible explanation being differences in the reaction kinetics among the various FAH species. Previous studies have demonstrated that both the chain length and degree of saturation of fatty acids influence the reactivity of their carboxylic acid groups. This is attributed to factors such as inductive effects, variations in electron affinity, and shifts in pKa values (61)(62). Analogously, such structural differences may also affect the reactivity of the hydroxamic acid group during acylation with pyridine-2-carbonyl chloride. Consequently, FAH species may undergo derivatization to varying extents, leading to differential increments in the signal intensities in mass spectrometric detection. This can be evaluated by performing separate derivatization reactions for each species and monitoring the extent of reaction over time using mass spectrometry. This approach allows for the determination of reaction kinetics for the individual species, thereby enabling

the identification of optimal conditions for the complete derivatization of all fatty acid hydroxamates.

It is also worth noting that a second derivatization agent, 4,4-dimethoxypiperidine, was evaluated in this study but was ultimately discarded due to its poor reaction yield (~11%) and the formation of numerous side-products, as observed via MS characterization. This further emphasizes the challenge in identifying suitable derivatization strategies for hydroxamic acids and highlights the value of the pyridine-2-carbonyl chloride approach.

The newly derivatization method was implemented in the analysis of S-acylated fatty acids released from the proteome of Neuro-2a (N2a) cells, a neuronal cell model relevant for neurodegenerative diseases such as CLN1. This new derivatization step significantly enhanced the detection signal of various FAH species, improving both the accuracy and resolution of their quantification. Moreover, contrary to the one-pot experiment, when tested on cells, the increment of intensity between the different species were very similar showing a positive consistency for accurate and quantitative results. The derivatized probe also enabled the detection of a broader range of fatty acids, including species such as C20:3 that were undetectable in their native FAH forms, thereby validating the enhanced analytical performance in a biological context. Furthermore, it was demonstrated that omitting the liquid-liquid extraction step improved reproducibility and signal consistency, especially for low-abundance samples while the remaining derivatization agent left in the sample did not interfere with the analysis of the derivatized FAH. Overall, the derivatized probe constitutes a robust and scalable strategy for the profiling of the S-acylome, with direct applications in the study of diseases involving dysfunctional protein acylation, such as neuronal ceroid lipofuscinosis.

In summary, while traditional derivatization strategies have dramatically improved the analysis of carboxylic acids, their applicability to hydroxamates remains limited. Our method addresses this gap by enabling efficient, reproducible, and sensitive detection of FAH a critical step forward in lipidomic analysis of S-acylated proteins. This methodological advance paves the way for more comprehensive and accurate profiling of the S-acylome, particularly in biological contexts where low-abundance or structurally diverse fatty acids may play critical roles in disease mechanisms.

Due to the limited time available for the development of this project, several critical steps remain to be addressed in order to fully validate and optimize a derivatization strategy suitable for the lipidomic analysis of S-acylation using hydroxylamine. First, the acylation reaction with

pyridine-2-carbonyl chloride should be systematically optimized. This includes not only refining parameters such as reaction time, temperature, and pH, but also performing detailed kinetic studies for each FAH species. These studies are essential to ensure uniform reaction efficiency across all fatty acid hydroxamates, thereby supporting truly quantitative analysis. Second, a more comprehensive evaluation of the impact of derivatization on the analytical performance should be conducted. This would involve assessing potential shifts in retention time during liquid chromatography and any interference or enhancement effects in electrospray ionization (ESI) and time-of-flight (TOF) mass spectrometry. Finally, for complete method validation and standardization, key analytical parameters, including linearity, limits of detection (LOD) and quantification (LOQ), intra- and inter-day precision, and analyte stability should be rigorously tested across a broader panel of FAH species. This will ensure consistency in sensitivity and quantification, regardless of fatty acid chain length or saturation, and establish the method as a robust tool for high-precision S-acylation profiling.

7. BIBLIOGRAPHY

1. S. Mesquita F, Abrami L, Linder ME, Bamji SX, Dickinson BC, van der Goot FG. Mechanisms and functions of protein S-acylation. Vol. 25, Nature Reviews Molecular Cell Biology. Nature Research; 2024. p. 488–509.
2. Qu M, Zhou X, Wang X, Li H. Lipid-induced s-palmitoylation as a vital regulator of cell signaling and disease development. Vol. 17, International Journal of Biological Sciences. Ivyspring International Publisher; 2021. p. 4223–37.
3. Hu L, Tao Z, Wu X. Insights into auto- S -fatty acylation: targets, druggability, and inhibitors. RSC Chem Biol. 2021;2(6):1567–79.
4. Lin DTS, Conibear E. ABHD17 proteins are novel protein depalmitoylases that regulate N-Ras palmitate turnover and subcellular localization. Elife. 2015 Dec 23;4.
5. Remsberg JR, Suciu RM, Zambetti NA, Hanigan TW, Firestone AJ, Inguva A, et al. ABHD17 regulation of plasma membrane palmitoylation and N-Ras-dependent cancer growth. Nat Chem Biol. 2021 Aug;17(8):856–64.
6. Kadry YA, Lee JY, Witze ES. Regulation of EGFR signalling by palmitoylation and its role in tumorigenesis. Open Biol. 2021 Oct 6;11(10).
7. Pei Z, Xiao Y, Meng J, Hudmon A, Cummins TR. Cardiac sodium channel palmitoylation regulates channel availability and myocyte excitability with implications for arrhythmia generation. Nat Commun. 2016 Jun 23;7(1):12035.
8. Ernst AM, Syed SA, Zaki O, Bottanelli F, Zheng H, Hacke M, et al. S-Palmitoylation Sorts Membrane Cargo for Anterograde Transport in the Golgi. Dev Cell. 2018 Nov;47(4):479-493.e7.
9. Zmuda F, Chamberlain LH. Regulatory effects of post-translational modifications on zDHHC S-acyltransferases. Journal of Biological Chemistry. 2020 Oct;295(43):14640–52.
10. Zhao L, Zhang C, Luo X, Wang P, Zhou W, Zhong S, et al. CD36 palmitoylation disrupts free fatty acid metabolism and promotes tissue inflammation in non-alcoholic steatohepatitis. J Hepatol. 2018 Sep;69(3):705–17.
11. Du K, Murakami S, Sun Y, Kilpatrick CL, Luscher B. DHHC7 Palmitoylates Glucose Transporter 4 (Glut4) and Regulates Glut4 Membrane Translocation. Journal of Biological Chemistry. 2017 Feb;292(7):2979–91.
12. Kharbanda A, Walter DM, Gudiel AA, Schek N, Feldser DM, Witze ES. Blocking EGFR palmitoylation suppresses PI3K signaling and mutant KRAS lung tumorigenesis. Sci Signal. 2020 Mar 3;13(621).

13. Yao H, Lan J, Li C, Shi H, Brosseau JP, Wang H, et al. Inhibiting PD-L1 palmitoylation enhances T-cell immune responses against tumours. Nat Biomed Eng. 2019 Mar 25;3(4):306–17.

14. Lu W, Wang J, Li Y, Tao H, Xiong H, Lian F, et al. Discovery and biological evaluation of vinylsulfonamide derivatives as highly potent, covalent TEAD autopalmitoylation inhibitors. Eur J Med Chem. 2019 Dec;184:111767.

15. Vetrivel KS, Meckler X, Chen Y, Nguyen PD, Seidah NG, Vassar R, et al. Alzheimer Disease Aβ Production in the Absence of S-Palmitoylation-dependent Targeting of BACE1 to Lipid Rafts. Journal of Biological Chemistry. 2009 Feb;284(6):3793–803.

16. Ho GPH, Ramalingam N, Imberdis T, Wilkie EC, Dettmer U, Selkoe DJ. Upregulation of Cellular Palmitoylation Mitigates α-Synuclein Accumulation and Neurotoxicity. Movement Disorders. 2021 Feb 26;36(2):348–59.

17. Virlogeux A, Scaramuzzino C, Lenoir S, Carpentier R, Louessard M, Genoux A, et al. Increasing brain palmitoylation rescues behavior and neuropathology in Huntington disease mice. Sci Adv. 2021 Apr 2;7(14).

18. Spinelli M, Fusco S, Mainardi M, Scala F, Natale F, Lapenta R, et al. Brain insulin resistance impairs hippocampal synaptic plasticity and memory by increasing GluA1 palmitoylation through FoxO3a. Nat Commun. 2017 Dec 8;8(1):2009.

19. Yokoi N, Fukata Y, Sekiya A, Murakami T, Kobayashi K, Fukata M. Identification of PSD-95 Depalmitoylating Enzymes. The Journal of Neuroscience. 2016 Jun 15;36(24):6431–44.

20. Gorinski N, Bijata M, Prasad S, Wirth A, Abdel Galil D, Zeug A, et al. Attenuated palmitoylation of serotonin receptor 5-HT1A affects receptor function and contributes to depression-like behaviors. Nat Commun. 2019 Sep 2;10(1):3924.

21. Busquets-Hernandez C, Ribo S, Gratacos-Batlle E, Carbajo D, Tsiotsia A, Blanco-Canosa JB, et al. Quantitative analysis of protein lipidation and acyl-CoAs reveals substrate preferences of the S-acylation machinery. Chem Sci. 2024 Jul 9;15(32):12845–55.

22. Resh MD. Fatty acylation of proteins: The long and the short of it. Vol. 63, Progress in Lipid Research. Elsevier Ltd; 2016. p. 120–31.

23. Schulte-Zweckel J, Dwivedi M, Brockmeyer A, Janning P, Winter R, Triola G. A hydroxylamine probe for profiling: S-acylated fatty acids on proteins. Chemical Communications. 2019;55(75):11183–6.

24. Nůsková H, Serebryakova M V., Ferrer-Caelles A, Sachsenheimer T, Lüchtenborg C, Miller AK, et al. Stearic acid blunts growth-factor signaling via oleoylation of GNAI proteins. Nat Commun. 2021 Jul 28;12(1):4590.

25. Liang X, Nazarian A, Erdjument-Bromage H, Bornmann W, Tempst P, Resh MD. Heterogeneous Fatty Acylation of Src Family Kinases with Polyunsaturated Fatty Acids Regulates Raft Localization and Signal Transduction. Journal of Biological Chemistry. 2001 Aug;276(33):30987–94.

26. Nůsková H, Serebryakova M V., Ferrer-Caelles A, Sachsenheimer T, Lüchtenborg C, Miller AK, et al. Stearic acid blunts growth-factor signaling via oleoylation of GNAI proteins. Nat Commun. 2021 Jul 28;12(1):4590.

27. Schmidt MF, Schlesinger MJ. Fatty acid binding to vesicular stomatitis virus glycoprotein: a new type of post-translational modification of the viral glycoprotein. Cell. 1979 Aug;17(4):813–9.

28. Muszbek L, Laposata M. Covalent modification of proteins by arachidonate and eicosapentaenoate in platelets. J Biol Chem. 1993 Aug 25;268(24):18243–8.

29. Hang HC, Geutjes EJ, Grotenbreg G, Pollington AM, Bijlmakers MJ, Ploegh HL. Chemical Probes for the Rapid Detection of Fatty-Acylated Proteins in Mammalian Cells. J Am Chem Soc. 2007 Mar 1;129(10):2744–5.

30. Martin BR, Cravatt BF. Large-scale profiling of protein palmitoylation in mammalian cells. Nat Methods. 2009 Feb 11;6(2):135–8.

31. Wang Y, Yang W. Proteome-Scale Analysis of Protein S-Acylation Comes of Age. J Proteome Res. 2021 Jan 1;20(1):14–26.

32. Martin BR, Cravatt BF. Large-scale profiling of protein palmitoylation in mammalian cells. Nat Methods. 2009 Feb;6(2):135–8.

33. Wan J, Roth AF, Bailey AO, Davis NG. Palmitoylated proteins: purification and identification. Nat Protoc. 2007;2(7):1573–84.

34. Forrester MT, Hess DT, Thompson JW, Hultman R, Moseley MA, Stamler JS, et al. Site-specific analysis of protein S-acylation by resin-assisted capture. J Lipid Res. 2011 Feb;52(2):393–8.

35. Percher A, Thinon E, Hang H. Mass-Tag Labeling Using Acyl-PEG Exchange for the Determination of Endogenous Protein S-Fatty Acylation. Curr Protoc Protein Sci. 2017 Aug 1;89:14.17.1-14.17.11.

36. Zhou B, Wang Y, Yan Y, Mariscal J, Di Vizio D, Freeman MR, et al. Low-Background Acyl-Biotinyl Exchange Largely Eliminates the Coisolation of Non-S-Acylated Proteins and Enables Deep S-Acylproteomic Analysis. Anal Chem. 2019 Aug 6;91(15):9858–66.

37. Ji G, Wu R, Zhang L, Yao J, Zhang C, Zhang X, et al. Global Analysis of Endogenously Intact S-Acylated Peptides Reveals Localization Differentiation of Heterogeneous Lipid Chains in Mammalian Cells. Anal Chem. 2023 Sep 5;95(35):13055–63.

38. Keenan EK, Bareja A, Lam Y, Grimsrud PA, Hirschey MD. Cysteine S-acetylation is a post-translational modification involved in metabolic regulation. 2024 May 21;

39. Mohammadzadeh F, Hosseini V, Mehdizadeh A, Dani C, Darabi M. A method for the gross analysis of global protein acylation by gas–liquid chromatography. IUBMB Life. 2019 Mar 30;71(3):340–6.

40. Sorek N, Akerman A, Yalovsky S. Analysis of protein prenylation and S-acylation using gas chromatography-coupled mass spectrometry. Methods Mol Biol. 2013;1043:121–34.

41. Dai X, Shen L. Advances and Trends in Omics Technology Development. Front Med (Lausanne). 2022;9:911861.

42. Wilm M. Principles of electrospray ionization. Mol Cell Proteomics. 2011 Jul;10(7):M111.009407.

43. Ho CS, Lam CWK, Chan MHM, Cheung RCK, Law LK, Lit LCW, et al. Electrospray ionisation mass spectrometry: principles and clinical applications. Clin Biochem Rev. 2003;24(1):3–12.

44. Yu Y, Le HH, Curtis BJ, Wrobel CJJ, Zhang B, Maxwell DN, et al. An Untargeted Approach for Revealing Electrophilic Metabolites. ACS Chem Biol. 2020 Nov 20;15(11):3030–7.

45. Haron MJ, Jahangirian H, Silong S, Yusof NA, Kassim A, Rafiee-Moghaddam R, et al. Benzyl and Methyl Fatty Hydroxamic Acids Based on Palm Kernel Oil as Chelating Agent for Liquid-Liquid Iron(III) Extraction. Int J Mol Sci. 2012 Feb 16;13(2):2148–59.

46. Poole CF. Derivatization in liquid chromatography. In: Liquid Chromatography. Elsevier; 2017. p. 39–68.

47. Gallagher PT, Gilmore J. Other Acyloxy Compounds. In: Comprehensive Organic Functional Group Transformations. Elsevier; 1995. p. 181–229.

48. Yang WC, Adamec J, Regnier FE. Enhancement of the LC/MS analysis of fatty acids through derivatization and stable isotope coding. Anal Chem. 2007 Jul 15;79(14):5150–7.

49. Qi BL, Liu P, Wang QY, Cai WJ, Yuan BF, Feng YQ. Derivatization for liquid chromatography-mass spectrometry. Vol. 59, TrAC - Trends in Analytical Chemistry. Elsevier B.V.; 2014. p. 121–32.

50. Johann T, Keth J, Bros M, Frey H. A general concept for the introduction of hydroxamic acids into polymers. Chem Sci. 2019;10(29):7009–22.

51. Mantzourani C, Kokotou MG. Liquid Chromatography-Mass Spectrometry (LC-MS) Derivatization-Based Methods for the Determination of Fatty Acids in Biological Samples. Vol. 27, Molecules. MDPI; 2022.

52. Tayama E, Naganuma N, Iwamoto H, Hasegawa E. Double axial chirality promoted asymmetric [2,3] Stevens rearrangement of N-cinnamyl L-alanine amide-derived ammonium ylides Electronic Supplementary Information Contents. 2014.

53. Couturier M, Tucker JL, Proulx C, Boucher G, Dubé P, Andresen BM, et al. 5,5-Dimethyl-1,4,2-dioxazoles as versatile aprotic hydroxamic acid protecting groups. Journal of Organic Chemistry. 2002 Jul 12;67(14):4833–8.

54. Schulz A, Kohlschütter A, Mink J, Simonati A, Williams R. NCL diseases - clinical perspectives. Biochim Biophys Acta. 2013 Nov;1832(11):1801–6.

55. Itagaki R, Endo M, Yanagisawa H, Hossain MA, Akiyama K, Yaginuma K, et al. Characteristics of PPT1 and TPP1 enzymes in neuronal ceroid lipofuscinosis (NCL) 1 and 2 by dried blood spots (DBS) and leukocytes and their application to newborn screening. Mol Genet Metab. 2018 May;124(1):64–70.

56. Gao J, Chen X, Ma T, He B, Li P, Zhao Y, et al. PEG-Ceramide Nanomicelles Induce Autophagy and Degrade Tau Proteins in N2a Cells. Int J Nanomedicine. 2020;15:6779–89.

57. Xu Y, Liang P, Rashid H ur, Wu L, Xie P, Wang H, et al. Design, synthesis, and biological evaluation of matrine derivatives possessing piperazine moiety as antitumor agents. Medicinal Chemistry Research. 2019 Oct 20;28(10):1618–27.

58. Esteves H, Xavier T, Lajnef S, Peyrot F, Lefèvre G, Prestat G, et al. Iron-catalyzed intramolecular C(sp 3)-H lactonization of hydroxamate derivatives promoted by a 1,5-HAT.

59. Wessel D, Flügge UI. A method for the quantitative recovery of protein in dilute solution in the presence of detergents and lipids. Anal Biochem. 1984 Apr;138(1):141–3.

60. Bligh EG, Dyer WJ. A RAPID METHOD OF TOTAL LIPID EXTRACTION AND PURIFICATION. Can J Biochem Physiol. 1959 Aug 1;37(8):911–7.

61. Vysotsky YB, Kartashynska ES, Vollhardt D, Fainerman VB. Surface p Kaof Saturated Carboxylic Acids at the Air/Water Interface: A Quantum Chemical Approach. Journal of Physical Chemistry C. 2020 Jun 25;124(25):13809–18.

62. Osatiashtiani A, Durndell LJ, Manayil JC, Lee AF, Wilson K. Influence of alkyl chain length on sulfated zirconia catalysed batch and continuous esterification of carboxylic acids by light alcohols. Green Chemistry. 2016;18(20):5529–35.

8. ANNEXES

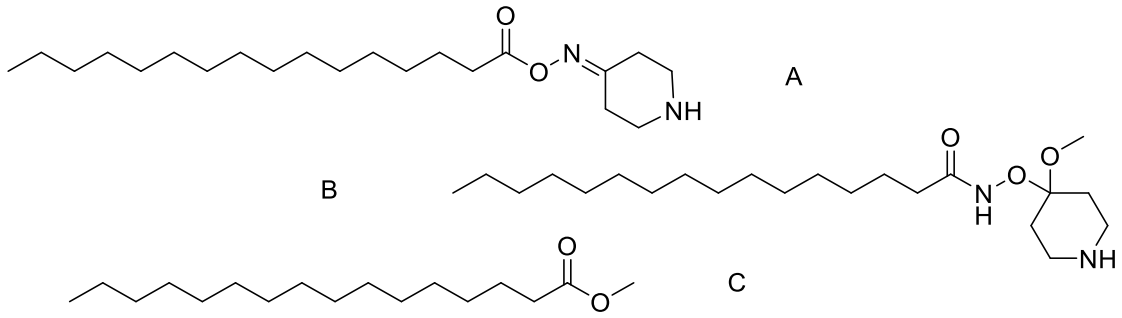

Annex 1: Side products formed during the derivatization of C16:0 FAH with 4,4-dimethoxypiperidine.

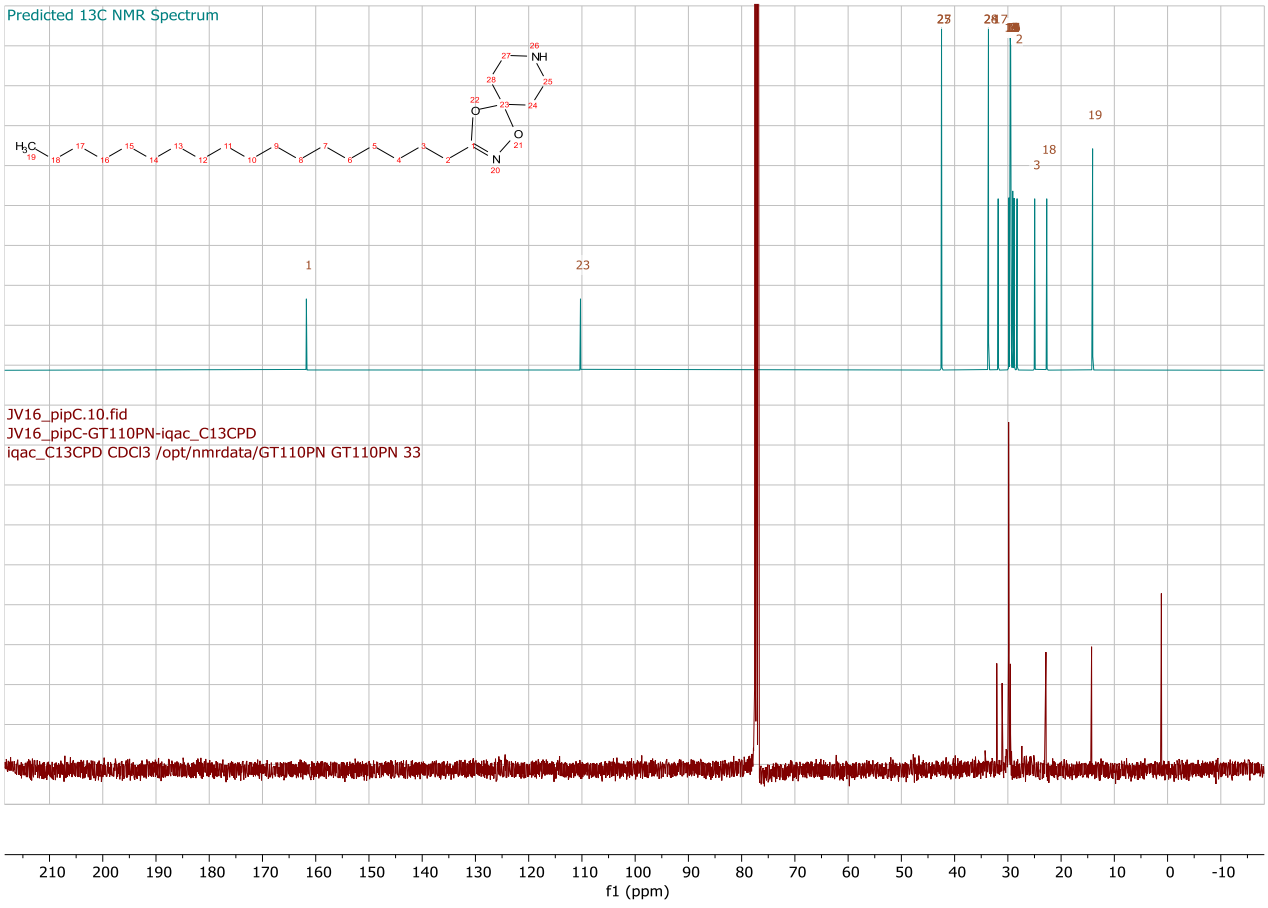

Annex 2: 13C NMR spectrum of the derivatized product with 4,4-dimethoxypiperidine (red) compared to its predicted spectrum (blue).

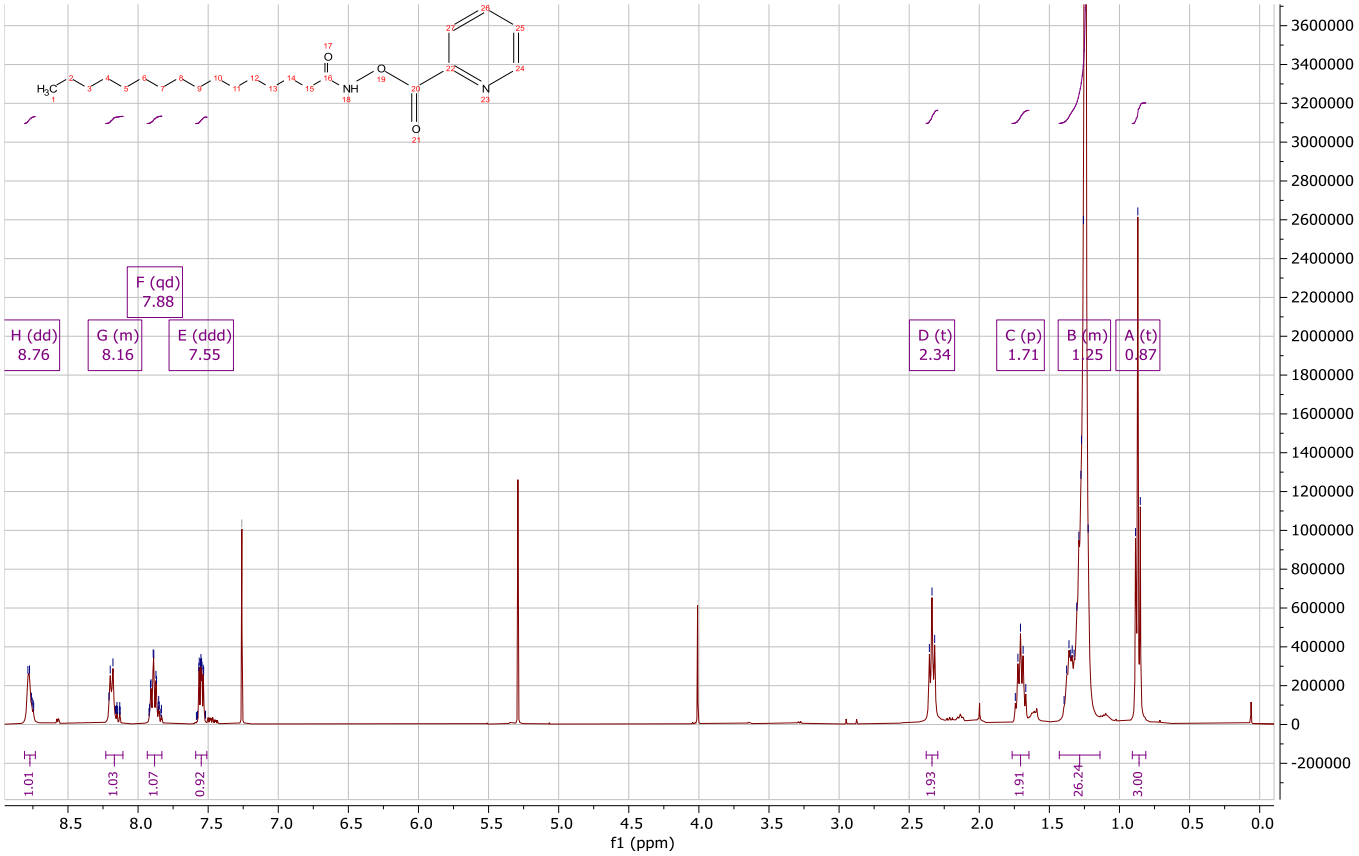

Annex 3: 1H NMR spectrum of the derivatized product with pyridine-2-carbonyl chloride.

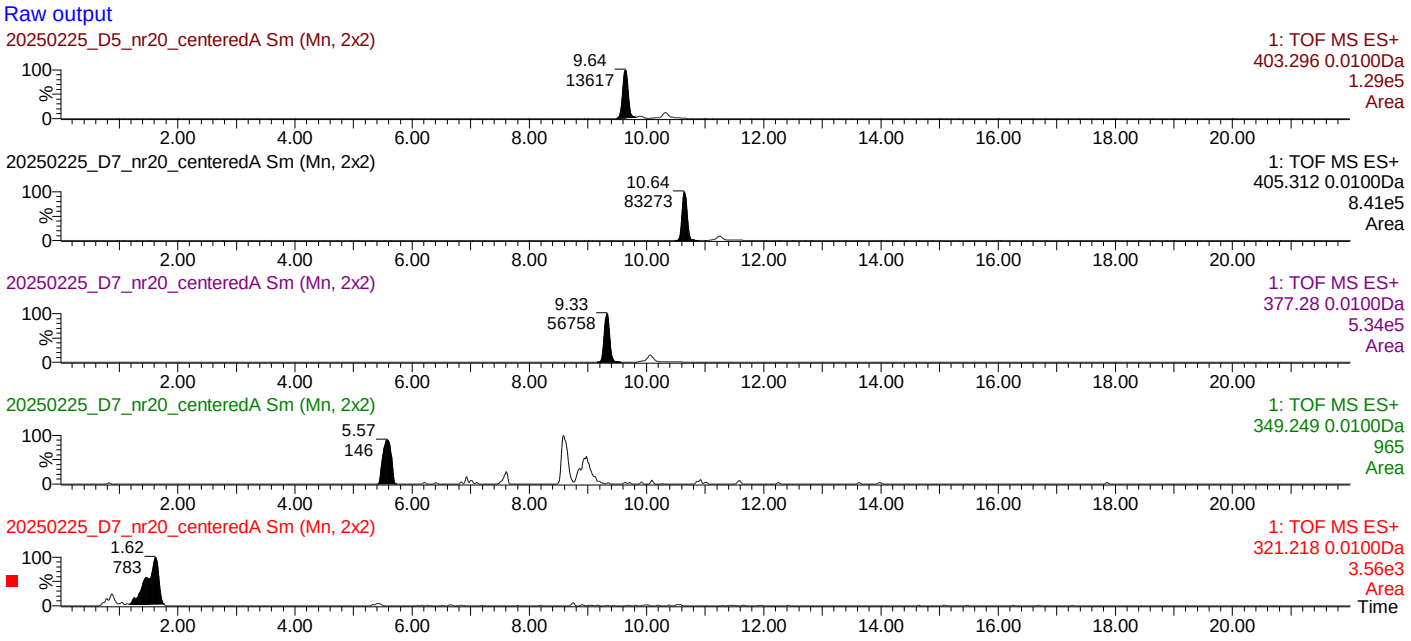

Annex 4: Chromatographic spectrum of derivatized FAH from N2a cell line S-acylome. Retention time and area of the signal can be seen for C12:0, C14:0, C16:0, C18:0, C18:1.